Science Advances
AAAS

advances.sciencemag.org/cgi/content/full/4/12/eaav0280/DC1

Supplementary Materials for

Radiocarbon re-dating of contact-era Iroquoian history in northeastern North America

Sturt W. Manning*, Jennifer Birch, Megan A. Conger, Michael W. Dee, Carol Griggs, Carla S. Hadden, Alan G. Hogg, Christopher Bronk Ramsey, Samantha Sanft, Peter Steier, Eva M. Wild

*Corresponding author. Email: sm456@cornell.edu

Published 5 December 2018, *Sci. Adv.* **4**, eaav0280 (2018)
DOI: 10.1126/sciadv.aav0280

The PDF file includes:

Supplementary Materials and Methods

Archaeology

In the mid-second millennium CE (all dates in this paper are CE) Iroquoian societies of northeastern North America developed a semi-sedentary settlement system whereby villages were occupied for an estimated (typical) ~10–50 years before being abandoned and relocated (*3, 4, 8, 14, 17*). Villages and communities were usually relocated within the same drainage, although more distant migrations also took place. The complex occupational histories of individual and sequential sites include evidence for processes of migration, aggregation, and the fission and fusion of community segments, permitting still-finer reconstructions of settlement dynamics. A general sequence of social, economic and political change has been identified (Table 1; *3, 14, 22*) including settlement patterns that progress through pre-coalescent, coalescent, and post-coalescent phases. The chronology and relative sequence has been derived from the absence and then presence (from the 16th century onwards) of European trade goods, from changes in the material culture and in particular ceramic design sequences, through examination of settlement patterns, and from a small number of ^{14}C dates (Table 1)—with the plateau in the ^{14}C calibration curve in the 16th century regarded as problematic and creating dating ambiguity—in the period before sustained and intensive European contact in the 17th and 18th centuries (*3, 4, 8, 13–17, 22, 34, 50–57*).

In the Rouge River-West Duffins drainage the Wendat community coalescent phase is represented by the sites of Draper (Borden designation: AlGt-2) (*58*) and Spang (AlGt-66) (*59, 60*). These sites are much larger than earlier (pre-coalescent) sites in the sequence. Draper is a 4.2ha village surrounded by a multi-row defensive palisade. The palisade was expanded on five separate occasions to incorporate new clusters of aligned longhouses. The presence of fragmented human bone in midden deposits and burials exhibits evidence for violent conflict and attests to a climate of advanced hostility that likely prompted local aggregation. The maximal population at Draper is estimated at approximately 1,800 persons (*14, 61*). It has been assumed that the Draper community relocated as a whole, first to Spang, and then to Mantle (site name as published (*14, 61*), renamed Jean-Baptiste Lainé in 2011) (AlGt-334) (*4, 14*). All three sites are

of a similar size and analyses of the agricultural catchments surrounding each site make it highly unlikely that the local area was capable of supporting two such populations concurrently (*14).* Spang is a 3.4ha village where limited excavation has revealed portions of longhouses and a five-row palisade (*59*). Recent geophysical prospection suggests the site layout may have included a central plaza (*60*), similar to that identified in the early phase of the Mantle site (*14*). The relative order of the sites is considered to be Draper and then Spang primarily because of chronologically-significant changes in ceramic decoration: in particular Huron incised types increase from 14% at Draper to 41% at Spang (*16*). The seriation of ceramic design sequences is well established for south-central Ontario, however, it is only loosely tied to absolute dates; this is especially the case for the later prehistoric sequence due to the reliance on trade good chronologies (*51–53*). No European trade goods have been reported from either site and hence traditionally both are placed, in sequence, within the period ~1450–1500 (*14*) (Table 1).

Subsequently, the community is assumed to have moved then to the Mantle site (*14*). The palisaded portion of the Mantle site has been completely excavated and its occupational history studied in detail (*14, 61*). That work suggests a more completely integrated community than was the case at Draper (*3, 14*). The early phase of the village plan exhibits a pre-planned layout where houses were arranged in a radial alignment around a single plaza. After a period of initial occupation, the palisade was contracted and the plaza filled with new structures. Mantle is placed later than the Draper and Spang sites in the relative ceramic seriation because incised decoration increases further (~60%) and neck decoration declines (~41–45% at Draper and Spang to ~2% at Mantle) (*16, 61*). The accepted date for the site is placed within ~1500–1550 particularly because of the recovery of two rolled copper beads and an iron fragment, all determined to be of European origin (*14, 61*). Within the traditional trade goods chronology, an occupation prior to 1550 was understood to only be possible if the iron fragment originated from the Basque presence on the Atlantic coast (*14).* Sample materials for ^{14}C dating were selected from features associated with early, middle, and late phases of the Mantle site's occupation *(14, 61).*

We also consider the Warminster (BdGv-1) site because it has been argued to have a potential direct historical association. Samuel de Champlain wrote an account of his visit in 1615–1616 to

an Arendarhonon (Wendat Rock Nation) village that he names as Cahiagué which would be located in modern Ontario (*5, 62*) and, while not conclusive and sometimes debated, the Warminster site has been argued to be Cahiagué (*1, 11, 12, 63–66*). Warminster is essentially a double village. It consists of two palisaded sections, located approximately 165m apart. The north village is 3.4ha in size and the south village 2.6ha. Seven complete longhouses and portions of 13 more were reported from the northern village (*64*). Similarities in the material culture assemblages recovered from each section of the site suggest that they were occupied contemporaneously (*4*). European metals and hundreds of glass trade beads have been identified at the site (*64*). A date in the range ~1600–1630 is usually given since the glass beads are overwhelmingly of glass bead period 2 types *(67)*. However, the glass bead dates are not entirely independent, since the exact dates assigned for the beginning and end of each glass bead period partly depend on a decision of whether or not Cahiagué = Warminster (*12, 64, 66, 67*). We ^{14}C-dated materials from this site to see, therefore, whether the ages were at least compatible with the approximate date ranges variously ascribed within the first two-three decades of the 17th century, or more specifically, the Champlain association in 1615–1616. If a ^{14}C-based chronology for the site can offer closely comparable dates for this approximately historically dated case, then we may assume that a ^{14}C-based chronology is also relevant for the late prehistoric cases from the coalescent and post-coalescent periods in the Rouge River-West Duffins drainage. The materials dated from Warminster comprise a wooden post (*Larix laricina*) from House 4 associated with Feature 13 (Cat #27442), a sample of bean (*Phaseolus* sp.) from Feature 16B in House 4, a sample of wild plum (*Prunus americana*) from Feature 12 in House 4, and two maize (*Zea mays*) samples from House 9 Feature 30C and House 5 Feature 1. We interpret the wood post as likely from a support for a bench or bunk line. The extant sample lacks the original outer tree-rings (an unknown number of rings to original bark are no longer present on the sample). The current last preserved tree-ring of the sample (see fig. S4) thus sets a TPQ for the human use of this wood as a post, and we assume that this last preserved tree-ring therefore also safely acts as a TPQ for the short-lived plant remains found both within the same house (House 4) and likely the other houses at the site.

Re-considering the basis of current trade goods chronologies

We note in the main text that the appearance and distribution of European trade goods have in existing work usually formed the basis of chronology-building from the mid-16th century onwards in northeastern North America, and so in turn underlie analyses of all aspects of social, economic, demographic, health and political change (*1–4 , 13, 14, 17, 18, 68*). It has been argued that scraps of European metals appear on Iroquoian sites in the mid-16th century and are later followed by glass beads, copper kettles, and other goods which were traded to and otherwise acquired by Indigenous individuals and groups (*13, 14, 20, 22, 67, 69, 70*). The types represented and the quantities present of European materials on Indigenous sites have been used to construct timelines such as the glass bead chronology (*19–21, 67, 69*), or to make assumptions about the chronological ordering of sites based on occurrences and frequencies of European goods (*12–14, 22*). However, these frameworks are implicitly based on the assumption that trade goods were distributed in a distance- and time-transgressive manner. Critical examination of the material record (with the caveat that available temporal resolution is often not of sub-century resolution) to the contrary suggests substantial site and regional variations across time and space. Contemporary perspectives on contact in the 16th and early-17th centuries recognize that participation in and access to trade networks varied. This resulted in differential distributions of European-derived goods within and among Iroquoian communities (*13, 42, 43, 45, 69–72*), including the outright rejection of European goods and influences in some cases (ref. 6 vol. 15: 15–22), rendering such trade good chronologies suspect. Notably, it was recently demonstrated that access to European copper differed among Wendat nations, and that individual communities controlled the trade in and availability of metals, particularly in the early contact period (*72).* More widely, there is now a rethinking of contact processes and Indigenous consumption of foreign materials across North America. Such studies invariably identify complicated histories of differences both within (e.g. variability amongst lineages and by rank), and among, Indigenous communities (*23*). Thus we argue for an alternative timeframe based on independent evidence (^{14}C), avoiding interpretative assumptions and logic transfers.

In general, it is important to note the fundamental differences between absolute versus relative chronologies, and, in turn, the very different status of timeframes derived from science-based

dates and empirically derived chronologies, versus dates based solely on relative chronology and so hypotheses and estimates that lack a quantified or demonstrable basis. Science-based dates come from measurements of physical processes (within errors), while archaeological and historical knowledge which is directly informative for dating derives from observations of stratigraphic relationships and similar known process or sequence observations or information (e.g. a known series of rulers (*40*)). Bayesian chronological modelling provides a mathematically coherent framework for combining such absolute and directly relevant relative chronological data. The contrast is with dates and chronologies derived from hypotheses, and assumptions, whereby calendar dates are at some point estimated for, or attached to, objects, assemblages or contexts. Although these estimated dates may subsequently become standard through repeated use and practice in a field of study, they lack a solid foundation. There is no secure basis, either in calendar time, nor understood physical or known processes or relationships. For example, an object, or technology, or style may be approximately associated with a date or period in one (historical) context (e.g. Europe in this case). But how, and when, this object, technology or style subsequently reached another very different context (various places in North America in this case), and why or when it subsequently became part of the archaeological record, introduce an unknown and potentially substantial period of time which may or may not be related to geographic distance. Nor can it be assumed that all social groups or regions engaged equally, or even at all, both in terms of time, and also space. Thus an absence of evidence, whether from a perfect or imperfect archaeological record, is not necessarily a temporal signifier. It is also key to observe that our timeframe should not merely be the result of trying to see if it is possible to fit new data to existing hypotheses. A rigorous chronology should be independent. We have thus kept our initial ^{14}C-based analyzes separate from the previous relative chronology assessments of site sequence in the case of the Draper, Spang and Mantle sites. In this way, the finding that our analysis of the ^{14}C data, and the existing relative archaeological investigations, both offer complementary information is mutually reinforcing, and hence important, and not merely circular.

In our study we have gathered well-contextualized samples and produced scientific dates, which, when subject to the laws of probability produce the stated results. The form of analysis we employ falls within the field of Bayesian statistics, founded on the famous Bayes' theorem

which, in the computer age, has rapidly become an important basis to various informed probability-based analyses in a myriad of fields including, since the 1990s, archaeology (*73, 74*) and especially via Bayesian chronological modelling (*26, 28, 31, 32, 33, 74, 75*). Bayesian statistics is not another form of arbitrary "interpretation", rather it is a comprehensive quantitative method permitting the interpretation of data conditional on associated (constraining) information. Terms such as "likely" have a specific meaning in probability, and we do not "interpret" dates with Bayesian analysis, we multiply and integrate probabilities and constraints to reach quantified solutions. Cogent criticism, if there is a disagreement with our work, should address the experimental set up, the samples, the measurements, the choice of priors, or the statistics. It is not legitimate to criticize such scientific data simply because they "don't fit" prior hypotheses. Legitimate opposing assessment needs to be supported by empirical evidence or identification of errors in method or the model parameters employed. It is no longer sufficient to say, for example, that the relative glass bead chronology, or the relative ceramic chronology, or available and again relative oral histories, offer better or more reliable evidence than a ^{14}C-based chronology. We acknowledge that the glass bead chronology is predicated upon calendar dates regarding when certain European materials were manufactured and transmitted to the New World (*42, 67*). However, we must also acknowledge issues of Indigenous agency, geopolitical dynamics, conflict, and cooperation that led to their transmission to communities hundreds of miles distant from places of direct Indigenous-European contact. The intervening (and variable) time-periods involved are not quantified, and introduce substantial unknowns. Such dynamics have begun to be investigated, but remain insufficiently understood and acknowledged in meta-narratives of Indigenous-European interactions in the early contact era (*13, 72*).

Radiocarbon Samples and Dates

The ^{14}C samples and dates employed in this study are set out in table S1 below. Dates run previously outside of this project were taken from the literature (*14*) or from the Canadian Archaeological Radiocarbon Database (CARD): http://www.canadianarchaeology.ca/. These latter data are employed as published/found. We did not employ one additional Beta date from the Mantle site (Beta-217158, 340±40 BP, see ref. 14) because we have no context information for this date, although the ^{14}C age is perfectly compatible with the other Mantle data on similar

maize samples. New dates were obtained on material directly sampled or obtained from museum or university collections held from the named sites. The samples comprised (i) short-lived plant remains (i.e. annual or sub-annual growth), (ii) wood-charcoal (see table S1), and (iii) the remains of a wooden post from House 4 at Warminster that was the subject of dendrochronological study prior to ^{14}C dating (see fig. S4). We obtained dates from a range of laboratories which each employed slightly differing procedures to test and ensure replicated and robust age estimates (see below). We observe no patterns of substantive differences between the results from the different laboratories within errors whether considering comparisons of ^{14}C dates on similar short-lived plant remains (all data on short-lived plant remains in table S1 except those with problematic $\delta^{13}C$ values—gray shaded—see below) from each site (fig. S1), nor when comparing the non-modelled independent calibrated age probabilities (green plots from short-lived plant remains) (figs. S2, S3). As one measure of the reasonable coherence of the collective dataset we may consider each of the sets of dates on short-lived samples from each of the four sites with the Combine function of OxCal (*32*). Here the dates are all assumed to refer to the same parameter (the date of the respective sites), but may be or are of different exact constituent ages (contrast the R_Combine function which assumes that a set of dates all refer to the same real ^{14}C age). The Combine function thus combines the calibrated calendar probability density functions (PDFs) for the given set and provides two measures (Chi-square test and the OxCal A_{comb} value) of whether the data are in fact plausibly similar. We note that we are not considering the further minor issue of correlated errors. We find for our data that in all four cases the sets of dates on the short-lived samples from each site can successfully combine at the 5% level (and so do not contain significantly different elements): (i) Draper χ^2 df10 T=6.52 <18.307 at 5% and OxCal A_{comb} = 137.8% > An = 21.3%; (ii) Spang χ^2 df7 T=12.724 <14.067 at 5% and OxCal Acomb = 35.5% > An = 25%; (iii) Mantle χ^2 df32 T=35.097 <45.671 at 5% (estimated by OxCal) and OxCal A_{comb} = 26.9% > An = 12.3%; and (iv) Warminster χ^2 df13 T=19.657 <22.362 at 5% and OxCal A_{comb} = 24.9% > An = 18.9%. Overall, only one date run some time ago taken from CARD (S-819 in table S1) on wood-charcoal from the Draper site appears to be an outlier (too recent), but even then the large measurement error permits it to be potentially acceptable. As we would anticipate, the ^{14}C dates on wood-charcoal samples (brown plots in figs. S2, S3) ranged from older (even occasionally much older, e.g. inner rings from a long-lived tree, or residual material) dates, to a majority of dates which offer relatively close TPQ estimates

for the archaeological contexts (figs. S2, S3). This observation and expectation is consistent with general ^{14}C interpretation principles (*76*) and thus modelling employing the Charcoal Outlier (*35*) or Charcoal Plus Outlier (*30*, *37*) models for such samples. The dates on the short-lived samples for each site group together within errors and may be expected to describe age estimates contemporary with their use (*76*). We summarize the dating approaches and any issues for each laboratory below.

(i) Groningen (GrM). The Groningen (CIO) routine pretreatment procedure for the samples in this project followed the ubiquitous acid-base-acid (ABA) framework (*77*). The first acid (HCl, 4% w/vol, 80^{o}C) step is employed to eliminate any geological carbonates that may have penetrated into the materials. The samples are then rinsed to neutrality with ultra-pure water. The second step involves the application of an alkaline solution (NaOH, 1% w/vol, RT) which dissolves any supramolecular polyphenols (mainly humic acids) that may have been absorbed from the soil. After another rinse to neutrality, a second acid step is employed (HCl, 4% w/vol, 80^{o}C) to ensure no atmospheric CO_2 absorbed during the alkaline phase remains in the reaction vessel. The samples are then rinsed to neutrality once more. For the wood samples, an additional aqueous oxidation step is also applied ($NaClO_2$,/H^+, 2.5% w/vol, 80^{o}C) to isolate the holocellulose fraction. This step is also followed by a final rinse to neutrality. The pretreated materials are then thoroughly dried. Approximately 3.5 mg aliquots of the charred seed and charcoal products, known as the reduced carbon fraction, and 5 mg of the holocellulose extracts, are then weighed into individual tin capsules for combustion in an Elemental Analyser (EA, IsotopeCube NCS, Elementar®). The EA is coupled to an Isotope Ratio Mass Spectrometer (IRMS, Isoprime® 100), which allows the $\delta^{13}C$ value of the sample to be measured, and a fully automated cryogenic system that traps the CO_2 liberated on combustion. When the run is complete, the individual reaction vessels are transferred to a graphitisation manifold, where a stoichiometric excess of H_2 gas (1: 2.5) is added, and the CO_2 gas is reduced to graphite over an Fe(s) catalyst. The graphite samples are then pressed into zinc cathodes, and their radiocarbon ratios measured by a MICADAS (IonPlus®) accelerator mass spectrometer (*78*). The quality of radiocarbon dates at the CIO is assured through the monitoring of subsidiary data relative to acceptance criteria, International Atomic Energy Agency (IAEA) reference and known-age sample measurement, and regular repetition of pretreatments on the same sample. Subsidiary

parameters include but are not limited to: sample pretreatment yields, %C on combustion, $\delta^{13}C$ and $\delta^{15}N$ values, and C:N ratios (bone collagen). Known-age standards of each of the main material types are taken through chemical pretreatment. The standards currently utilised include but are not limited to: the horse bone from the VIRI interlaboratory comparison; the Owen Buddleia modern charcoal standard (Oxford Radiocarbon Accelerator Unit); background wood from Kitzbuhel, Austria; and assorted dendrochronological tree-rings from the Dutch Cultural Heritage Agency. In addition, the CIO have prepared and supplied radiocarbon reference materials for the IAEA for several decades including standards IAEA-C3, IAEA-C7 and IAEA-C8. To date the CIO have obtained 30 measurements with the new MICADAS AMS on fully pretreated known-age samples (22 tree-ring, 8 bone). The average offset from expected values was 3±3 yr BP; 60.0% of results lay within 1SD of the expected value and 96.7% within 2SD.

(ii) Oxford (OxA). The organic samples dated for this project were subject to Acid-Base-Acid (ABA) sample pretreatment, target preparation, and Accelerator Mass Spectrometry (AMS) ^{14}C dating following standard published procedures and controls at the Oxford Radiocarbon Accelerator Unit (*79–81*). Isotopic fractionation has been corrected for employing the $\delta^{13}C$ values measured on the AMS—the quoted $\delta^{13}C$ values (table S1) were measured independently on a stable isotope mass spectrometer (±0.3‰ relative to VPDB). The Oxford laboratory maintains a known-age testing regime to assess on-going dating accuracy with details in previous publications (*40, 82*). These measurements were measured at the start of February 2016 and over the six-month period centering on this 01-11-2015 to 01-05-2016, a total of 50 measurements were made on known-age samples of wood and these demonstrated that 94% of the dates were within 2σ with a systematic bias of only 4.6±4.4 years relative to IntCal13. Other recent dating at Oxford on known-age wood samples from the UK with standard mid-latitude northern hemisphere spring-summer growing seasons from the second millennium CE (as comparable to the Ontario samples), including in the time period of this project, also demonstrate good agreement with the IntCal13 dataset (*40, 47, 48, 83*).

(iii) University of Georgia (UGAMS). The UGAMS Dates measured at the Center for Applied Isotope Studies (CAIS) at the University of Georgia were processed using the following

protocols and standard laboratory procedures (*84*). The samples were pre-treated using the acid/alkali/acid (AAA) method. Samples were placed in 1N HCl and heated to 80ºC for 1 hour to remove secondary carbonates and acid-soluble compounds; washed with 0.1 M NaOH to remove possible contamination by humic acids; and treated with dilute HCl a second time to remove atmospheric CO_2. Following each acid or alkali treatment the samples were washed in deionized water, centrifuged, and decanted. Samples were dried at 60ºC. For AMS analysis, the cleaned samples were combusted at 900°C in evacuated/sealed quartz ampoules in the presence of CuO. The resulting carbon dioxide was cryogenically purified from the other reaction products and catalytically converted to graphite (*85*). Graphite $^{14}C/^{13}C$ ratios were measured using the CAIS 0.5 MeV accelerator mass spectrometer and normalized using the Oxalic Acid I standard (NBS SRM 4990). To correct for isotopic fractionation, the sample $^{13}C/^{12}C$ ratios were measured separately using isotope ratio mass spectrometry (IRMS) and expressed as $\delta^{13}C$ with respect to PDB, with an error of less than 0.1‰. The quoted uncalibrated dates have been given in radiocarbon years BP (before 1950 CE), calculated using the Libby half-life of 5568 years. The error is quoted as one standard deviation and reflects both statistical and experimental errors. The quality of radiocarbon dates is assured through the monitoring of known-age standards, including Oxalic Acid I (NBS SRM 4990) and wood from the FIRI interlaboratory comparison (FIRI D,F), as well as anthracite background. We report an average pMC value of 104.65±0.26 from 65 measurements of full-sized OXI standards measured over a period of 6 months.

We note that in the case of one sample from Warminster, the *Prunus americana* (plum) sample from Feature 12, we carried out repeated and additional investigation and analyses (see table S2). It seemed that the original result, UGAMS-25451, was perhaps an apparent outlier (too old) versus the other dates from House 4 at Warminster, and we wished to better assess the likely appropriate radiocarbon age of this sample for this study. The other approaches and dates on this sample offer slightly later ages, but nonetheless all six dates may be regarded as plausible estimates of the same real ^{14}C age (weighted average 376±9 ^{14}C years BP) within 95% probability limits (see table S2). Moreover, if we consider the overall range of the ^{14}C dates $\pm 1\sigma$ that we have on short-lived plant materials from the Warminster site versus (i) the IntCal13 modelled calibration curve mid-point range and (ii) the range of the raw, constituent, data employed to construct IntCal13 (from http://intcal.qub.ac.uk/intcal13/), then we in fact see that

the calendar period we find as most likely for the Warminster site phase (see Fig. 2), somewhere between ~1585–1624, offers (uniquely) a range of ^{14}C ages that could in fact encompass all the Warminster values including UGAMS-25451 as only a minor over-estimation of the date of the marked wiggle in the ^{14}C curve to older ^{14}C ages ~1603–1607 (fig. S5).

(iv) Vienna (VERA). ABA sample pretreatment, target preparation and AMS ^{14}C dating were performed on the organic samples at the Vienna Environmental Research Accelerator following procedures described previously (*86*, *87*). For the samples VERA-6212 to VERA-6227 and the corresponding humic acids the combustion was slightly modified, i.e. Cu rods were added to the combustion tubes. All other samples were combusted in the standard way. Comparison of data from samples, where the modified combustion was applied, with dating results determined in a second dating run with sample splits combusted with the standard method (same VERA-numbers extended with 2) shows excellent agreement. Dates labelled HS represent the dating of the precipitated humic acids—extracted in the alkaline step (*88*); there is no evidence that these dates deviate from the ages determined on the fully treated samples (and so we employ them with the other ^{14}C dates). The two 'Cu' dates represent cases where Cu rods were added to the combustion tubes and to identify them for comparison with split samples without this addition (same VERA numbers without Cu) which were combusted with the standard method and measured in the same measurement run. The stated $\delta^{13}C$ values are determined with the AMS system and represent the $\delta^{13}C$ values of the graphitized carbon sample. Thus these values give information about the stable carbon isotopes fractionation in nature plus in the laboratory during sample processing and measurement. It is advantageous for isotope fractionation correction in ^{14}C dating also to include consideration of isotopic fractionation in the laboratory. Comparisons between ^{14}C measurements made at VERA versus those from Oxford, and elsewhere, and analysis of dates from VERA on known age samples, show good correspondence/quality (*27, 40, 89, 90*).

(v) Waikato (Wk). Wood samples were pretreated, combusted and graphitized in the University of Waikato AMS laboratory, with $^{14}C/^{12}C$ measurement by the University of California at Irvine (UCI) on a NEC compact (1.5SDH) AMS system. The pretreated samples were converted to CO_2

by combustion in sealed pre-baked quartz tubes, containing Cu and Ag wire. The CO_2 was then converted to graphite using H_2 and an Fe catalyst, and loaded into aluminum target holders for measurement at UCI. The samples were pretreated using a dilute acid/dilute alkali/dilute acid treatment (ABA). The routine procedure is 1M HCl at 80°C for 1hr; 1M NaOH at 80°C for 30 mins; 1M HCl at 80°C for 1 hr; 80°C, MilliQ™ water for 5 mins (pH>5), sonicated, then dried at 80°C. The NaOH treatments continues until the color is no longer transferred from sample to the liquid, with the number of treatments varying depending on the quantity and condition of the wood.

Bayesian Chronological Modelling

Our Bayesian chronological modelling employs the OxCal software (*32, 91, 92*) (specific version 4.3.2 dated 2017), and the IntCal13 ^{14}C calibration dataset as relevant to the mid-latitude northern hemisphere (*34*). Curve resolution was set at 1 year. We use capitalized forms of words such as Sequence, Phase, Boundary, Date, Span, Order to refer to OxCal terminology. The models and elements are described in the text, shown in Figs. 2–4, S6–S11, and the OxCal runfiles for Figs. 2–4, S8, S9 are listed in tables S5-S9 (Note: OxCal assumes that IntCal13, the current northern hemisphere ^{14}C calibration curve at the time of writing, is the calibration dataset to employ and this does not need to be specified.) Bayesian chronological modelling has become a widely employed method in archaeology, allowing robust more accurate and precise timeframes to be achieved, and, in particular, the quantification of the timing and tempo of both episodes and change (*26–33, 40, 74, 75, 91–94*).

In general terms we have data from the relatively short occupation, believed to be a couple to a few/several decades at most (*8, 14*), of several Iroquoian sites. We thus regard the data from each site as belonging to a Phase in OxCal (no order of elements within the Phase is assumed unless indicated; they are instead assumed to be a group of events randomly sampled from a uniform distribution between a start point termed a Boundary, and an end point termed a Boundary). We sought to employ the minimum of assumptions. To begin we treated each Phase entirely independently: no further assumptions were made as regards relationships between the sites.

Each Phase is thus bracketed by a start and end Boundary and run within its own independent Sequence in the generic form of:

```
Sequence()
  {
   Boundary();
   Phase()
   {
    R_Date("Radiocarbon Date1",X1,Y1)
    R_Date("Radiocarbon Date2",X2,Y2);
    …
   };
   Boundary();
  };
```

Where Radiocarbon Date 1, 2 … are the names or identifiers of ^{14}C dates and X1,Y1 and X2,Y2 are respective conventional ^{14}C ages and their stated measurement errors.

OxCal calculates a Probability Density Function (PDF) for each of these elements. Within the Phase we make two queries in all cases: (1) we use a Date command to query the PDF describing the Phase (i.e. the date of the site), and (2) we use the Span command to query the length of time in calendar years represented by the site in the model (we only report this for Sequence models, see tables 2, S3). We employ the Order function to determine the relative order of the Draper, Spang and Mantle sites (we compare the Date PDFs calculated for each separate Phase) having placed each of the separate site Phases within an over-arching (parent) Phase containing this Order query (table S4). In the analysis shown in Fig. 4 the known order or sequence of information from (i) the independent Order function examination (table S4), and (ii) the consistent assessment of the relative order of the sites determined from changes in archaeological traits (*3, 14–16*) is considered using the Sequence command to more closely resolve the chronology of the sites. We employ a Trapezoidal Boundary model to better reflect expected slightly overlapping ends and beginnings of the successive Phases within the sequence (*41, 92, 95*). The captions to Figs. 3 and S2 describe example OxCal model plots in full detail. All model

runs are very slightly different (with small variations typically of just a very few years at most among those runs with good convergence values of >95%, except sometimes the probabilities and dates vary more at the extremes and very low probability ends of long-tail distributions—an example of this is illustrated in fig. S10 contrasted with Fig. 3B, and see also fig. S11 comparing 10 different runs of the model in Fig. 3) and all models were run multiple times to ensure we report and show typical and thus reliable/robust outcomes with good convergence. Where there was a tree-ring sequenced set of ^{14}C dates (Fig. 2, fig. S4) we employed 'wiggle-matching' (*36, 96*) and the resultant TPQ estimate for the last extant (but clearly not original outermost) tree-ring was employed as a TPQ for the samples on short-lived plant material from the Phase (see the Warminster site case—and the runfile in table S5A, S5B).

Outlier analysis of the dates in the wiggle-match employed the SSimple Outlier model in OxCal (*35*). Outlier analysis to identify and down-weight possible outliers among the dates on short-lived (annual) plant matter (individual dates or R_Combine groupings) employed the General Outlier model in OxCal (*35*). Where ^{14}C dates were run on the very same short-lived sample (and so the real ^{14}C age being measured in each case should be the same) we considered a weighted average (*97*) using the R_Combine function in OxCal, but included an additional 8 years error term to allow for intra-annual variation (*38*). This procedure was followed as long as the R_Combine passed a Chi-Squared test at the 5% level, which was the case in all instances—with one exception (see below). For outlier assessment of the data in the R_Combine and the R_Combine product we used the SSimple Outlier model for the individual data and the General Outlier model for the R_Combine itself (following the coding examples in ref. 98). Outlier analysis is reported as, e.g., O:4/5, where the first number is the Posterior outlier probability and second number, 5, is the Prior outlier probability. The date is considered a possible outlier where the Posterior probability is greater than the Prior level of P=0.05 or 5% (i.e., the Posterior probability of being an outlier is above the acceptable level of 5% probability). For the Charcoal Outlier model (labelled as "IA" = Inbuilt Age in the runfiles in tables S6, S8, S9) and Charcoal Plus Outlier model the outlier value is always reported as 100:100. In six cases individual dates employed in the Fig. 3 model within an R_Combine (despite this passing a Chi-Square test) were flagged as minor possible outliers by the SSimple test (VERA-6286 O:8/5; OxA-33079 O:8/5; VERA-6215_2 O:12/5; VERA-6219 O:12/5; OxA-33082 O:16/5 and VERA-6217 O:6/5). We

considered the Fig. 3 and Fig. 4 models again without these six data and found negligible differences: see fig. S7, Table 2.

The one variation to the R_Combine approach outlined above concerned the Warminster site. In our first model we did as stated above and considered all the ^{14}C dates on the same two samples as two weighted averages (Figs. 2A, 2B). The data combine successfully and the model has good A_{model} and $A_{overall}$ values of typically around 90.2 and 93. Within the R_Combine for the plum sample, however, two dates, UGAMS-25451 and UGAMS-25451-r are identified by the SSimple Outlier model as likely outliers (with respective values of O:92/5 and O:19/5). If we re-run the same model but excluding these two dates, we nonetheless get a very similar result varying only a few years compared with Fig. 2B, with a Warminster Date Estimate now of 1580–1623 CE (68.2% hpd) and 1548–1645 CE (95.4% hpd)—the A_{model} is typically 95.1 and the $A_{overall}$ typically is 97.8. However, we also considered a second approach for the Warminster short-lived dates. While in two cases these were dates on the very same laboratory prepared sample (VERA-6309, VERA-6309_2), the other dates involved different pretreatments of the (same) samples and therefore might better be considered as independent measurements (even if of the same sample). Thus we ran an alternative model treating each of the ^{14}C dates on the Warminster plum and bean samples as independent dates. The Phase for the Warminster short-lived samples in this model thus had two independent sub-Phases, one with the dates on the plum sample and one with the dates on the bean sample, as well as two ^{14}C dates on different maize samples (see table S5B). We report the results in Fig. 2C. There are no outliers applying the OxCal General Outlier model for the run reported in Fig. 2C. However, one date, UGAMS-25451, has a very low OxCal agreement index value (A:5), which largely explains why this overall model had A_{model} and $A_{overall}$ values under 60 at typically 46.2 and 47.7. We thus tried a re-run of the Fig. 2C model (table S5B) excluding UGAMS-25451. The Warminster Date calculated is shown in Fig. 2D. The probability is very similar to that found in Fig. 2C. The model however now has satisfactory OxCal A_{model} and $A_{overall}$ values of 84.7 and 88.2 (from typical runs). Overall, we note that both models and variations reported in Figs. 2A-D and this paragraph produced very similar results for the Warminster Date Estimate. We thus regard this date estimate range as robust.

Where we included dates on wood-charcoal samples we assumed that they predated their find contexts. This is because the radiocarbon age of tree-rings reflects when the relevant tree-ring grew (the biological age) and when this material stopped exchanging carbon with the atmosphere. For other than bark or the outermost tree-ring, this age will be older than the archaeological context, thus providing a TPQ for the archaeological context of interest (*76*). If the tree species is long-lived and the tree-rings are from inner tree-rings, then this in-built age offset can be considerable (the so-called 'old-wood' problem (*99*)). To try to allow for this issue of in-built age for wood-charcoal samples, other than the wiggle-match (see above), we modelled them using either the Charcoal Outlier model (*35*) or a further adaptation in the Charcoal Plus Outlier model (*30, 37*). In each case the model selects shifts for the reported ages strongly biased towards possible younger ages. (Note: to use the Charcoal Plus Outlier model in OxCal the user needs first to create a Prior file with the probability distribution described in ref. 30 table S6 or ref. 37 Fig. 8).

In the case of the Spang and Mantle sites there is some internal phasing or order information. For Spang this is negligible, but one sample, comes from Midden 2 Level 4, which should be earlier than the other samples from Midden 2 Level 3. Unfortunately, there is just this one earlier sample and little information on real stratigraphic control for the site. Figure S8 considers this Spang Sequence. The runfile is in table S7. If the Level 4 sample is older and representative, then this model provides a clearer scenario with Spang dating in the mid-later 16th century (since we can rule out the 17th century probability because our other data show that this must belong with the Mantle site). The Mantle site which was fully excavated in considerable detail offers more indications of internal phasing (*14, 61*). We consider a model employing a sub-set of those samples which we believe are securely associated with the different phases of the site based on our (JB) best assessment of the excavation reports and analyses (*14, 61*). We define these internal phases (oldest to most recent) as: 1. 'Early', 2. 'Mid-Late', 3. 'Late', and 4. 'Very Late'. This Sequence model (employing the Charcoal Outlier model (*35*)) for Mantle is shown in fig. S9 with selected results in table S3, and the OxCal runfile is in table S8. The results are compatible with those treating Mantle as one combined Phase (compare with the overall Mantle date ranges in Figs. 3, S6, S7).

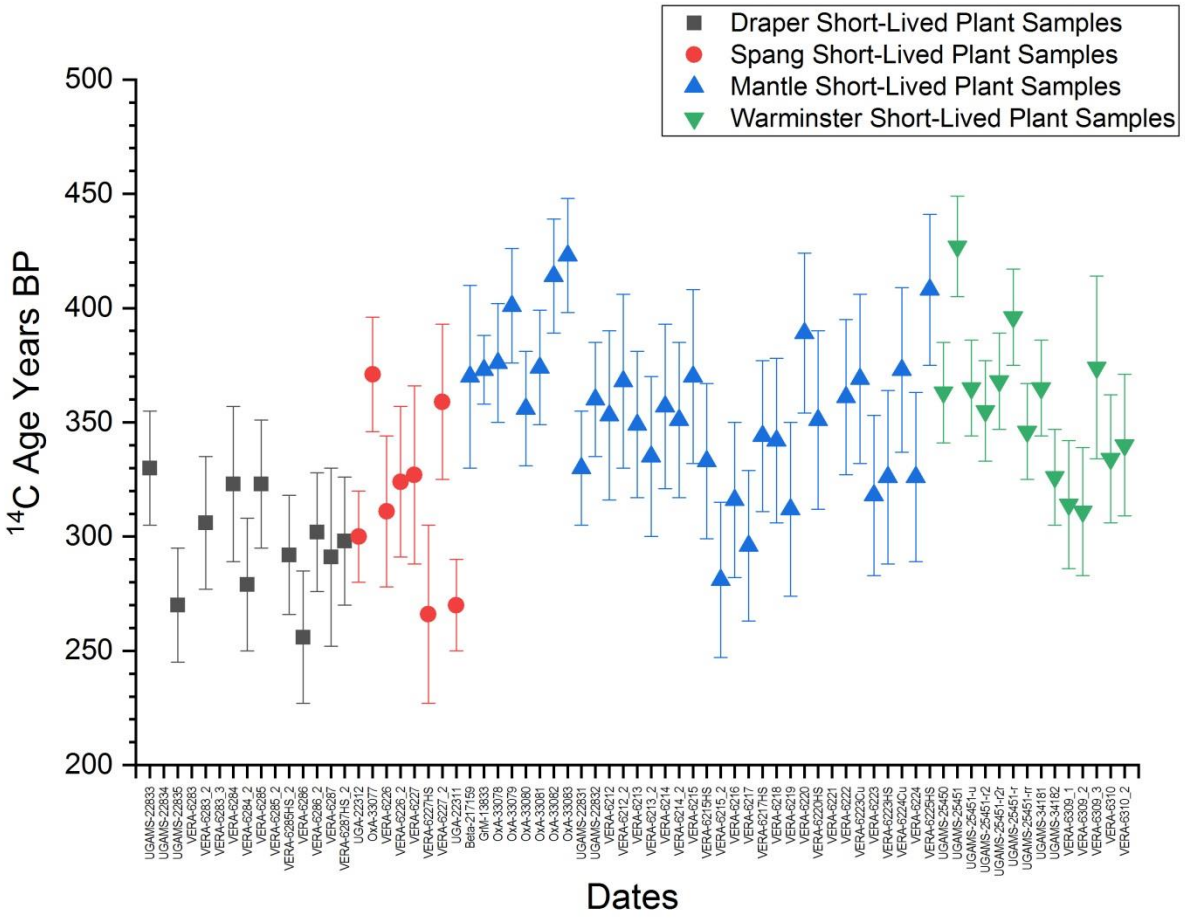

Fig. S1. A comparison of the ^{14}C ages [conventional radiocarbon years before the present (BP)] reported on samples of short-lived plant remains in table S1 by site (excluding the four dates with problematic $\delta^{13}C$ values—see table S1). All error bars are 1σ.

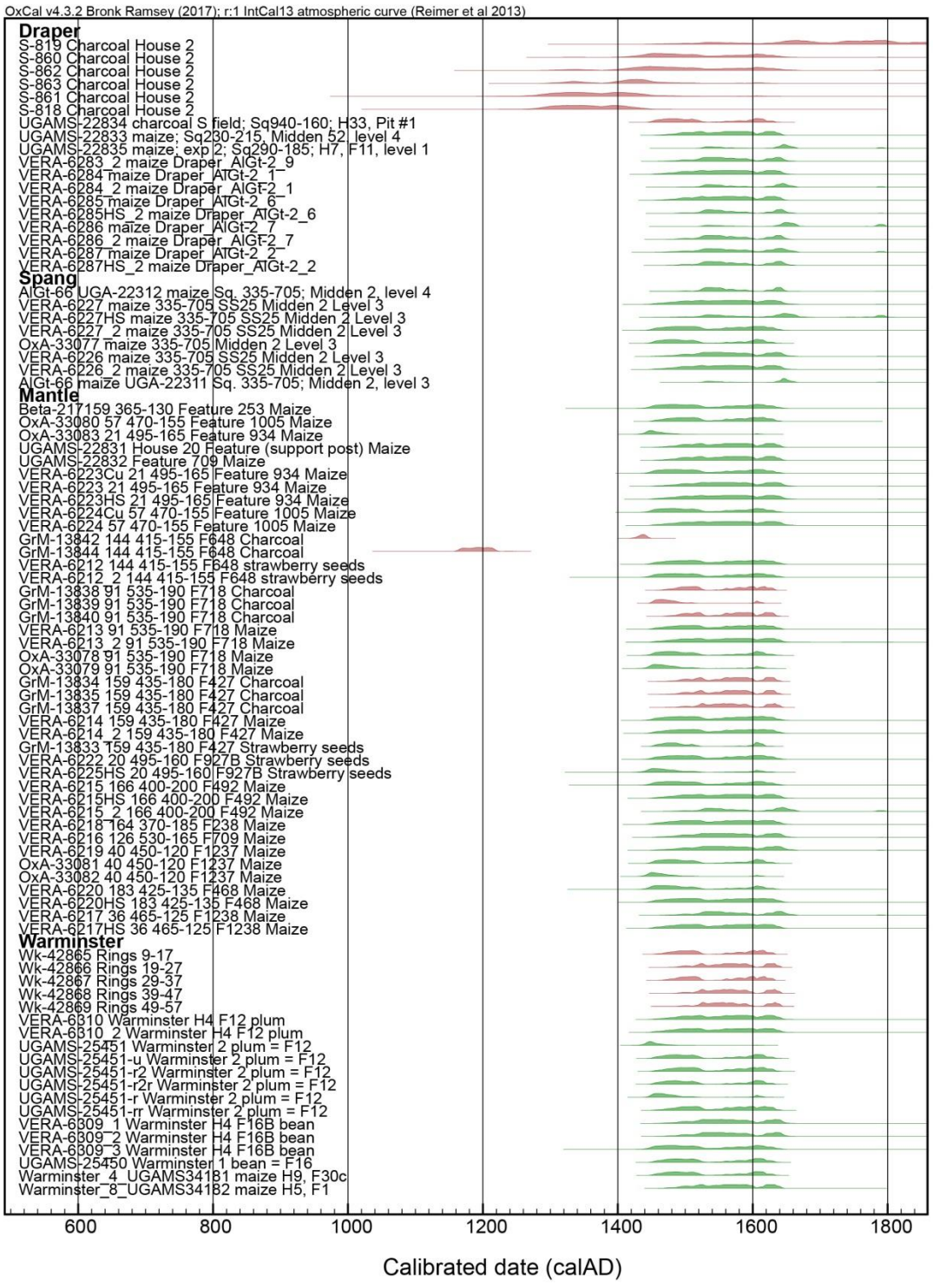

Fig. S2. The nonmodeled, individual, calibrated calendar dating probability ranges for the ^{14}C dates reported in table S1 (excluding the four with problematic $\delta^{13}C$ values—see table S1). Green plots = short-lived plant remains samples. Brown plots = wood charcoal samples. Data from OxCal 4.3 (*32*) and IntCal13 (*34*) with calibration curve set at 1 year.

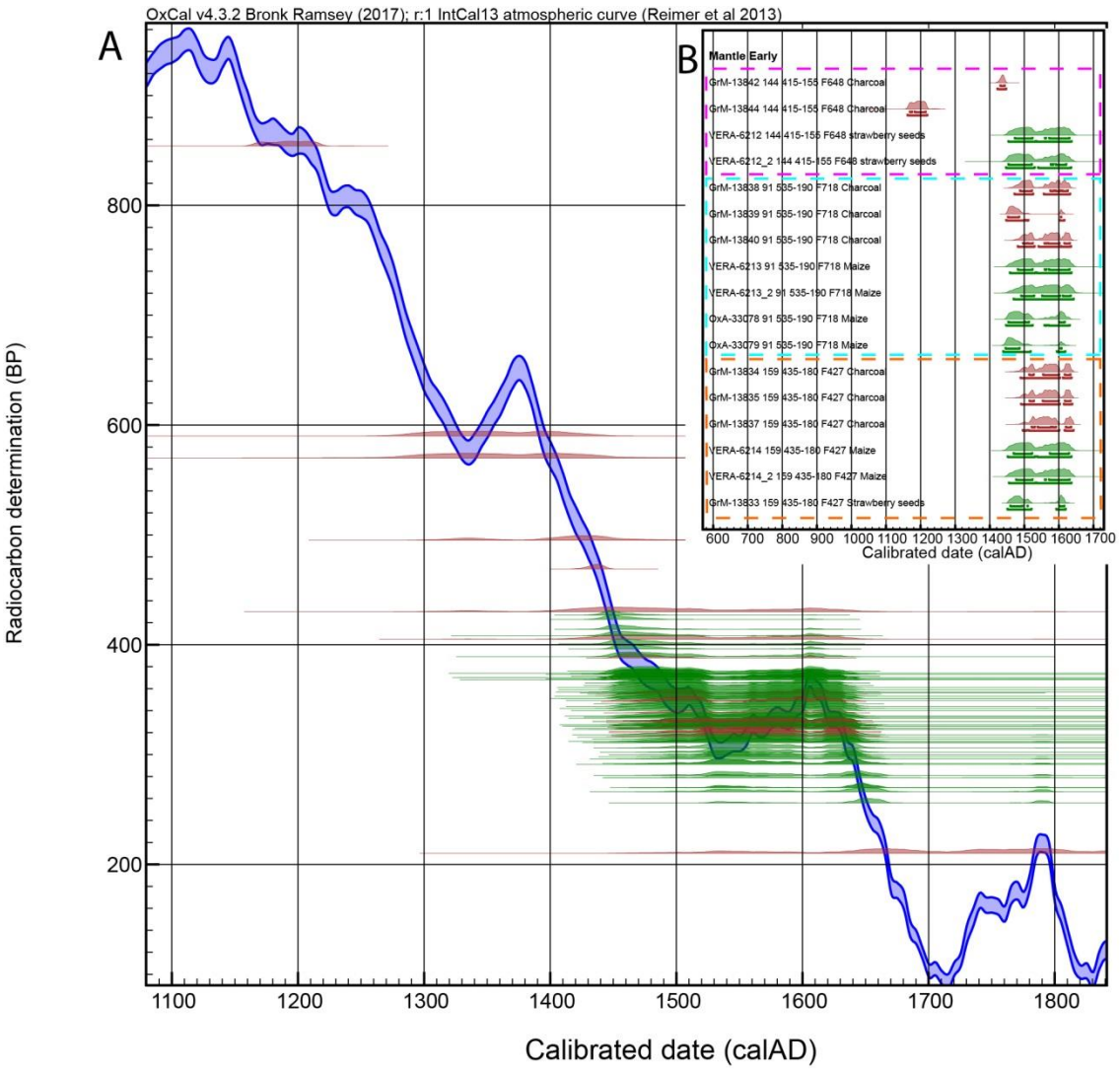

Fig. S3. The nonmodeled, individual, calibrated calendar dating probability ranges for the ^{14}C dates reported in table S1 shown against the IntCal13 calibration curve and the (nonmodeled) calibrated age probabilities for the subset of dates on samples just from Mantle early contexts. A. The non-modelled, individual, calibrated calendar dating probability ranges for the ^{14}C dates reported in table S1 (excluding the four with problematic δ^{13}C values—see table S1) shown against the IntCal13 calibration curve (1σ). B. The (non-modelled) calibrated age probabilities for the sub-set of dates on samples just from Mantle early contexts. The lines under each probability distribution indicate (upper, lower) the respective 68.2% and 95.4% ranges. Green plots = short-lived plant remains samples. Brown plots = wood charcoal samples. In B. the samples are from three early contexts at Mantle. The dates on the wood-charcoal samples (brown) should set TPQ for the dates on the short-lived (annual) plant material

(green). To resolve (since the probabilities for the samples overlap in most cases), the dates on the wood-charcoal samples must date from the mid-later 16th century and older, whereas the dates on the short-lived plant material must date later, and thus in the very late 16th century and especially very early 17th century (see Figs. 3, S9). Data from OxCal 4.3 (*32*) and IntCal13 (*34*) with calibration curve set at 1 year.

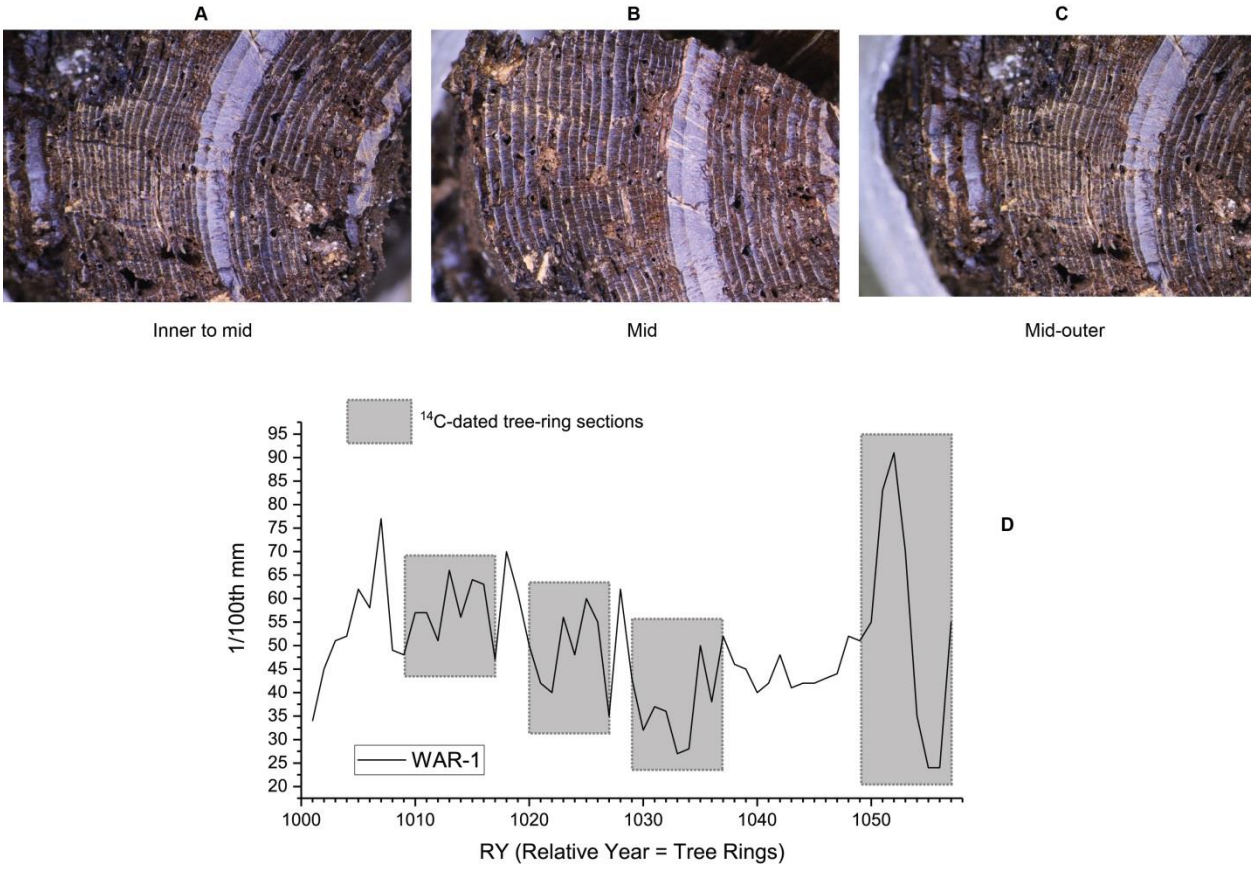

Fig. S4. Photos and ring-width measurements, WAR-1 sample. A-C: photos of the inner-to-mid, mid, and mid-to-outer parts of a transverse section across part of the WAR-1 sample (House 4 Feature 13 post), *Larix laricina*. D: ring widths (combining two measurements across different radii) in 1/100ths of a mm for the WAR-1 sample. Samples comprising the rings indicated by the gray boxes were employed for the dendro-^{14}C-wiggle-match dating (see Fig. 2).

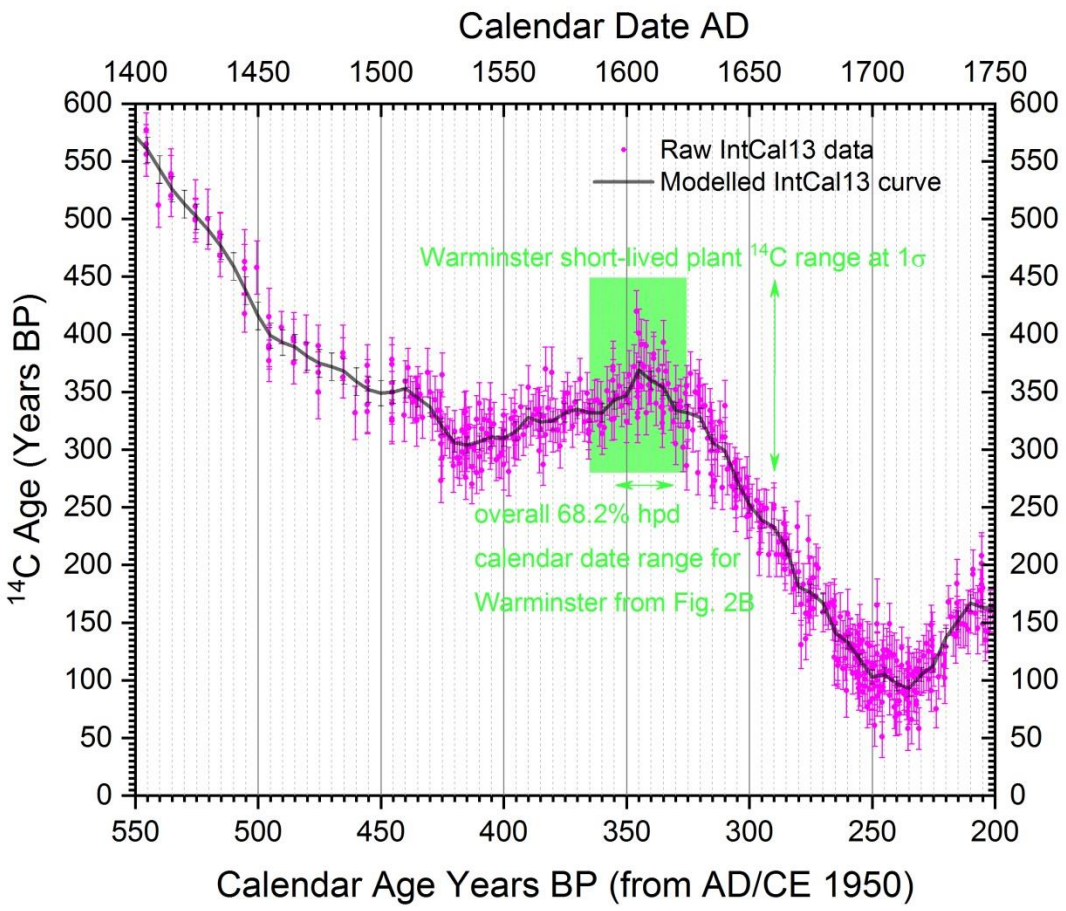

Fig. S5. Comparison of the ^{14}C range (overall 1σ) of the set of ^{14}C dates on short-lived plant remains from Warminster (see table S1) against the modeled (mid-point) and raw (constituent) IntCal13 (*34*) data (shown with 1σ errors) (raw data from: http://intcal.qub.ac.uk/intcal13/) placed within the calendar period, ~1596–1619, identified in the analysis reported in Fig. 2.

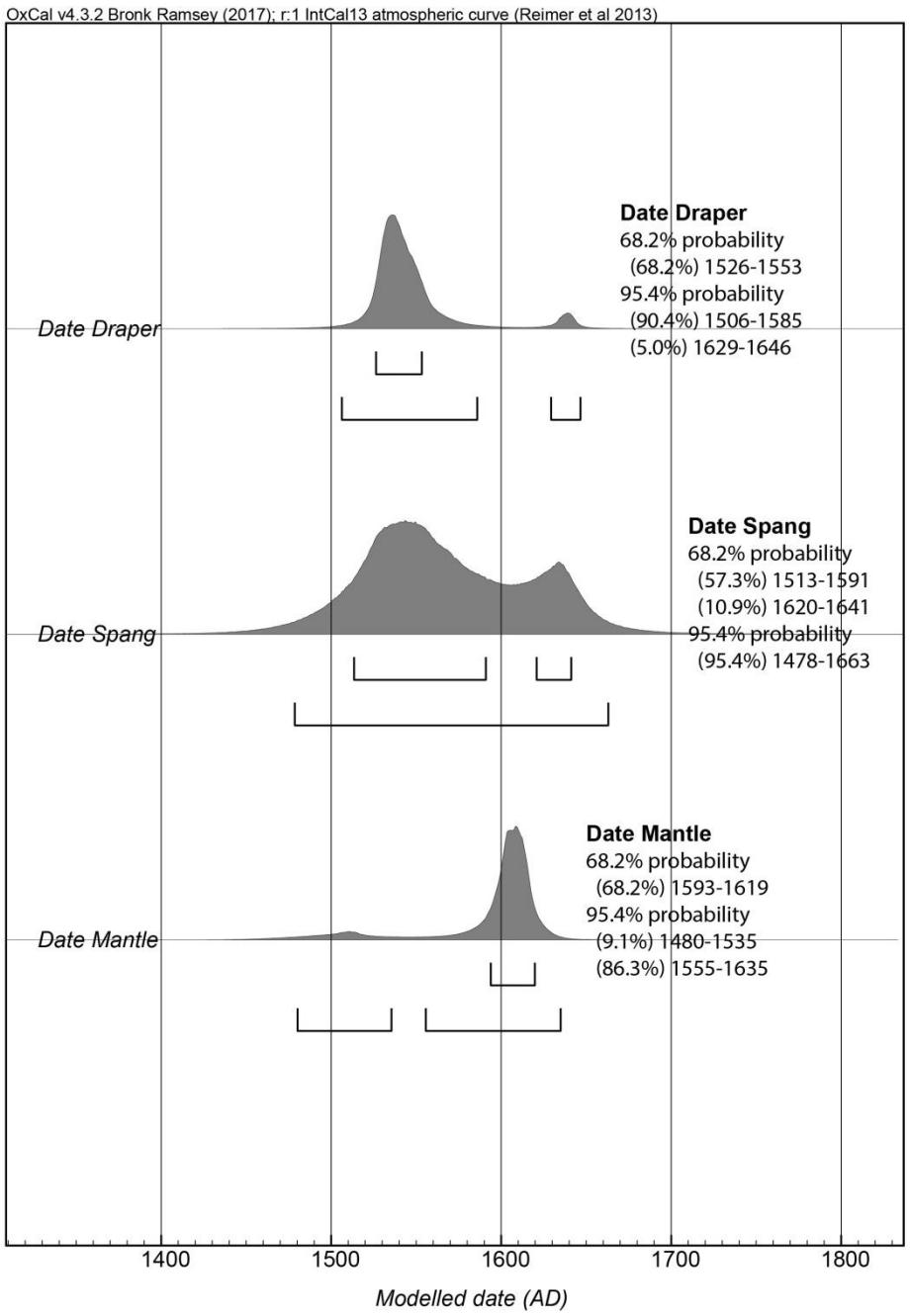

Fig. S6. Results from an alternative run of the dataset in Fig. 3 as summarized in Fig. 3B but using the Charcoal Plus Outlier model (*30, 37*). Typical A_{model} is 97.7 and $A_{overall}$ is 94.2. There is negligible difference versus the Fig. 3 model and results.

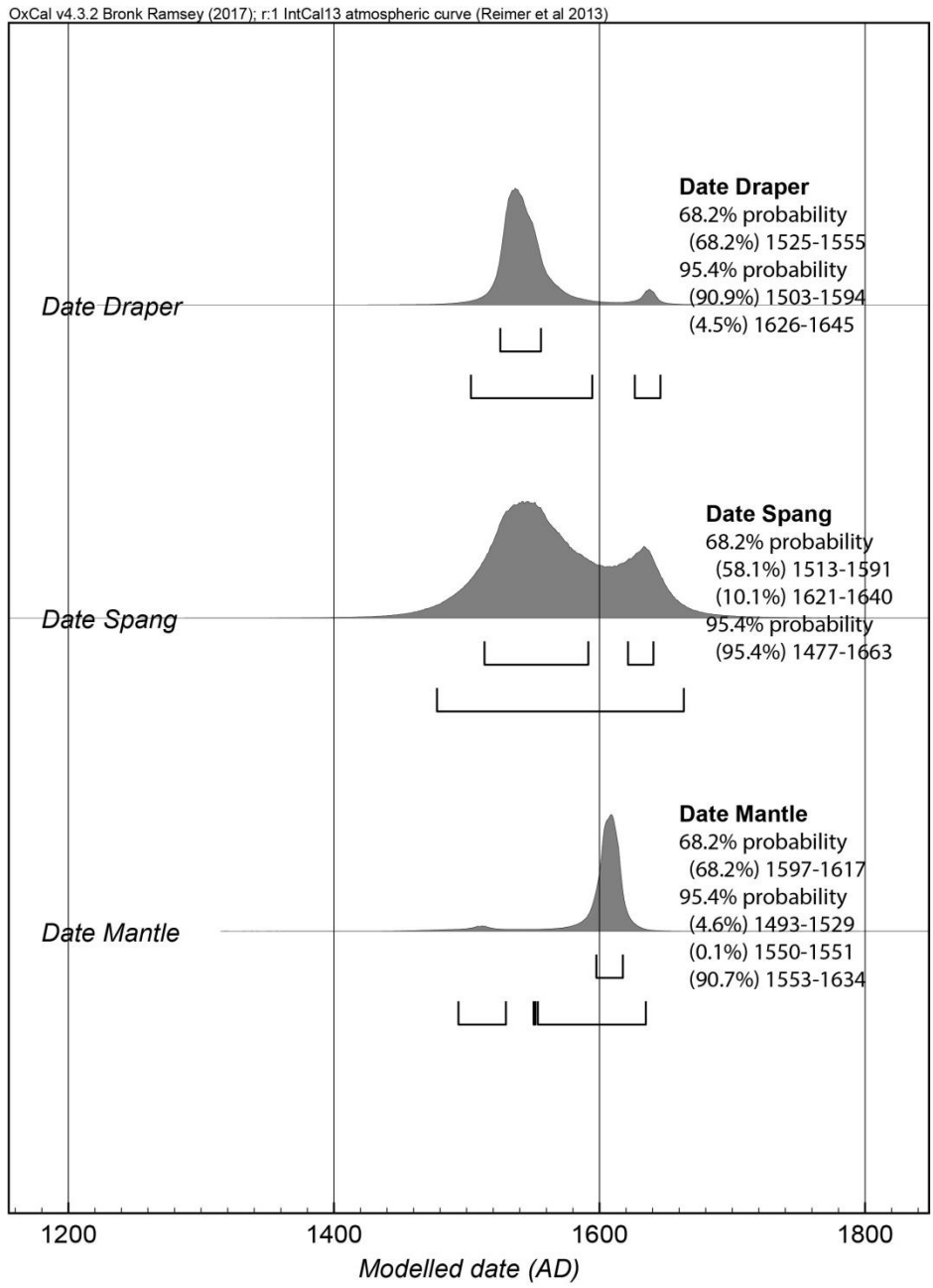

Fig. S7. Results from an alternative run of the dataset in Fig. 3 as summarized in Fig. 3B but after excluding the six minor possible outliers identified by the SSimple Outlier model in the various R_Combines (VERA-6286 O:8/5, OxA-33079 O:8/5, VERA-6215_2 O:12/5, VERA-6219 O:12/5, OxA-33082 O:16/5, and VERA-6217 O:6/5). This run, as Fig. 3 employs the Charcoal Outlier model (*35*).Typical values are A_{model} 122.5 and $A_{overall}$ 115. There is little difference compared to the results in Fig. 3B.

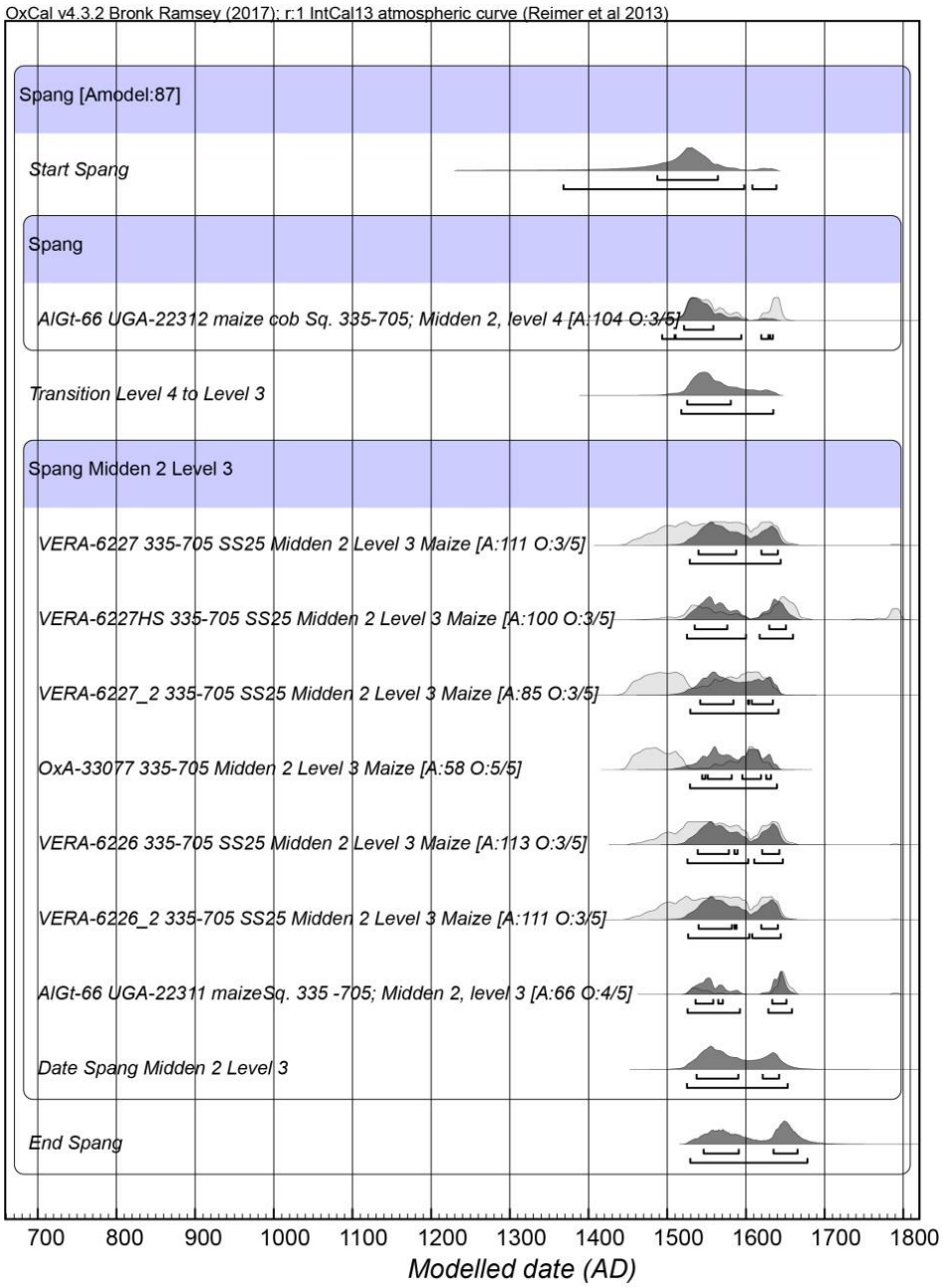

Fig. S8. Revised model of the Spang site data as a Sequence with the Midden 2 Level 4 date treated as earlier than the Phase of Midden 2 Level 3 dates. For the OxCal runfile, see table S7.

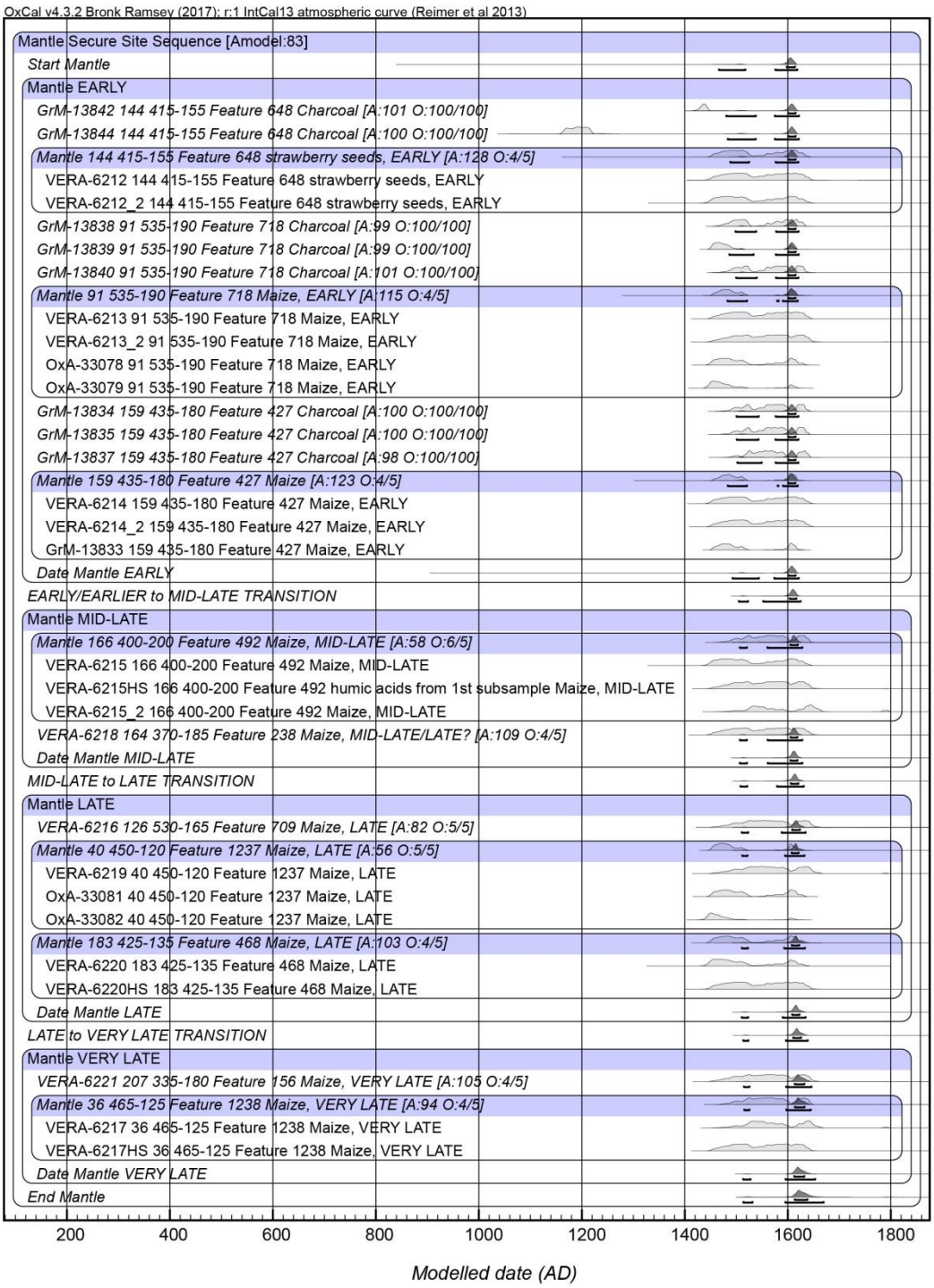

Fig. S9. Revised model of the Mantle site as a Sequence using those samples best associated with the intrasite phasing (*14*, *61*). For details of results see table S3. For the OxCal runfile see table S8.

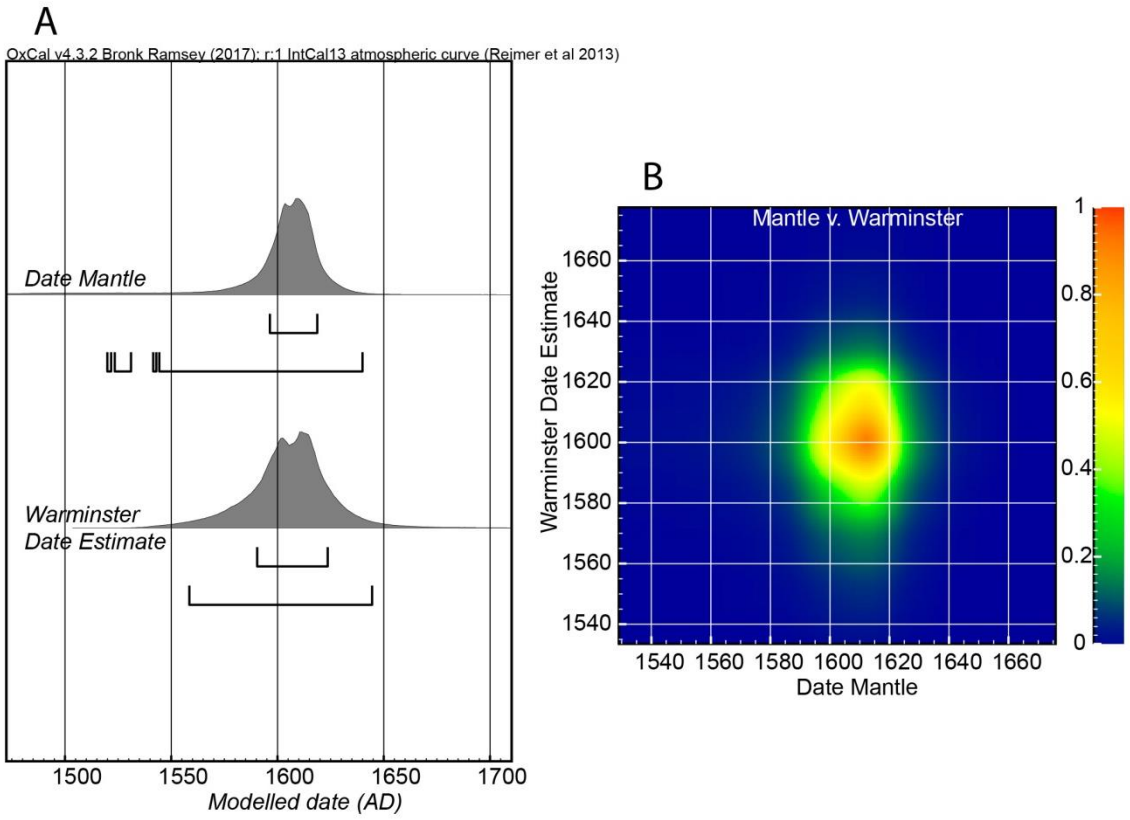

Fig. S10. Comparisons of the Warminster Date Estimate probability density function (PDF) from Fig. 2D with the Date Mantle PDF from Fig. 3. A. Plot showing the two PDFs on the same timescale for comparison. Note (as an example) that on the run shown here the earlier and unlikely late 15th-earlier 16th century CE date range for the Date Mantle PDF is a little different compared with the PDF shown in Fig. 3B. In Fig. 3B the date ranges at 95.4% probability were 1494–1533 (4.4%), 1545–1546 (0.1%) and 1548–1636 (90.9%); here they are instead 1519–1521 (0.1%), 1523–1531 (0.4%), 1541–1543 (0.1%) and 1544–1640 (94.8%). The main probability regions are of course very similar, with >90% probability 1548–1636 in both PDFs, but there is variation between the runs in the calculation of the unlikely extremes of this long-tail distribution (see also fig. S11). B. Correlation of the two PDFs employing the Correlation function of OxCal (*32*). Data from OxCal 4.3.2 and IntCal13 (*34*). We may observe from both A. and B. that it is quite likely the two sites were chronological contemporaries (or at least close), especially somewhere within the interval ~1595–1620.

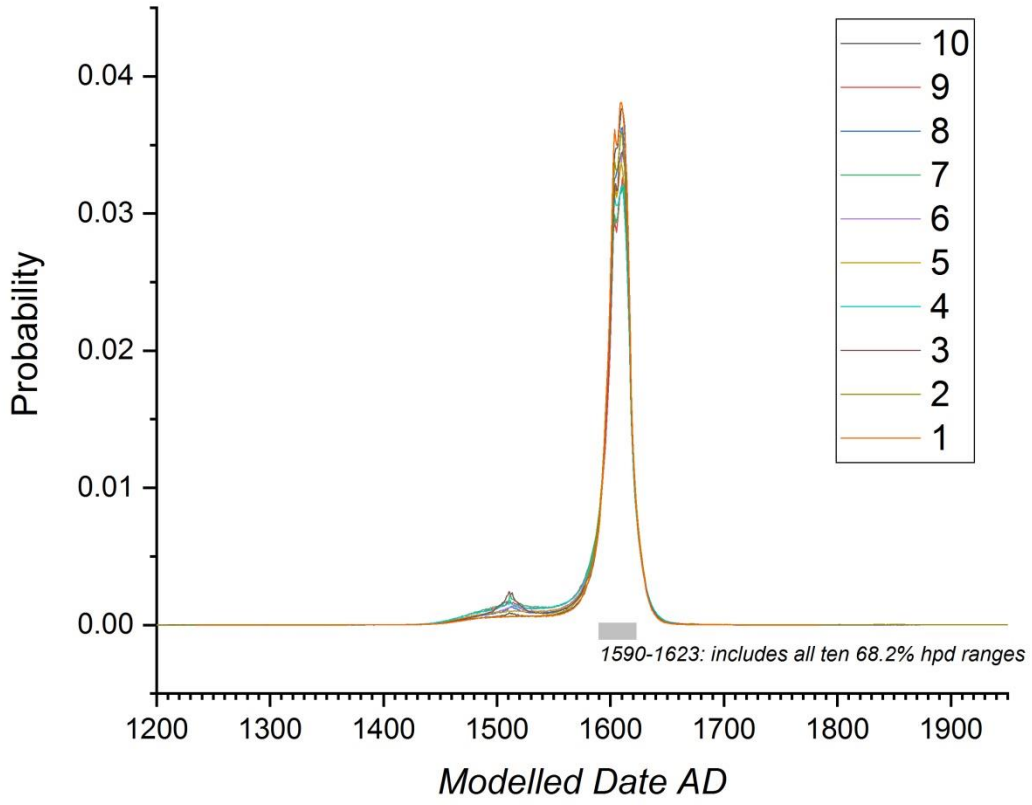

Fig. S11. Comparison of the PDFs for the Date Mantle estimate from 10 runs of the Mantle model in Fig. 3. This comparison illustrates the small variations possible between runs and especially in the low probability regions, but it also highlights that the main region of probability remains very similar across all runs and so is robust. The total limits of the 95.4% hpd ranges across the 10 runs vary from 1478/1488/1492/1493(x2)/1500 (x2)/1501//1504/1519 to 1637/1638(x2)/1639(x3)/1640(x3)/1641. As evident from the probability plots, there is more very minor variation in calculated probabilities among the different runs in the low probability region ~1470–1520 than elsewhere. The most likely 68.2% hpd ranges are very similar for all 10 runs with total limits varying only from 1590/1591(x2)/1593(x3)/1594(x2)/1595/1596 to 1618/1619(x2)/1620(x2)/1621(x2)/1622(x2)/1623.

Table S1. The samples and conventional radiocarbon dates used in this study. Samples labelled S- are taken from the Canadian Archaeological Radiocarbon Database (CARD: http://www.canadianarchaeology.ca/). Beta = Beta Analytic (date from ref. 14); GrM = Groningen AMS ^{14}C dates run on their MICADAS AMS; OxA = Oxford Radiocarbon Accelerator Unit; UGAMS = AMS dated samples from the Center for Applied Isotope Studies, The University of Georgia; VERA = AMS dates from the Vienna Environmental Research Accelerator; Wk = AMS dates with targets prepared at the Waikato Radiocarbon Dating Laboratory with the target run at the Keck Laboratory (UC Irvine). Maize or Corn = *Zea mays.* Strawberry = *Fragaria virginiana.* Wood charcoal samples marked with an asterisk (*) do not have species identifications. Wood charcoal species where known are listed. All the Beta, GrM, OxA, UGAMS, VERA and Wk dates are corrected for isotopic fractionation (*100*). Where known the δ^{13}C values for the samples are listed. The GrM and OxA values are from independent IRMS analyzes; the UGAMS δ^{13}C values were measured by IRMS and the quoted error is based on multiple analyses of internal standards; the VERA data are from the AMS values. Maize is a C4 plant and its δ^{13}C value is usually regarded as about -10±2‰ or -10±3‰ (*100*) although values reported in fact range a little more widely from about -8.7 to -15.7‰ (*101*). As clarified in the 1980s, ^{14}C dates on maize samples provide accurate ^{14}C ages as long as they have been appropriately corrected for isotopic fractionation (*102*). In four cases (VERA-6283, VERA-6283_3, VERA-6285_2 and VERA-6221; grey shaded cells) the δ^{13}C values for maize samples deviate, or are close to deviating, from the expected values. Although these δ^{13}C values are actually the values of the graphitized carbon (and not solely the maize sample), which were determined with the AMS system, the δ^{13}C values determined with the same method for the other maize samples clearly reflect the C4 plant isotopic signature. Therefore, these four dates were not included in our analysis (to clarify: 90 ^{14}C dates are listed in table S1 but we employ 86 ^{14}C dates in this study). Whether this effect is caused by a larger isotopic fractionation of the target carbon, or is due to other reasons, like some mix-up of the sample material either in the submitted sample (some C3 material present in the samples) or in the lab, both of which we believe is highly unlikely, must be left open (in the case of VERA-6285_2 we note that the sample available for this date was very small, thus additional fractionation in this measurement is more plausible). The Wk dates, with the targets run at the Keck laboratory (UC Irvine), do not have reported δ^{13}C values, but are corrected for isotopic fractionation. This reflects the policy of

the Keck laboratory not to release AMS-produced $\delta^{13}C$ values which always include fractionation. For details on sample pretreatments by each laboratory providing new dates for this study, see the Supplementary Materials text above.

Lab ID	Site	Sample ID	Mantle Intra-Site Sequence Phasing	Material	$\delta^{13}C$‰	SD	^{14}C Age BP	SD
S-819	Draper	House 2		Wood Charcoal*			210	80
S-860	Draper	House 2		Wood Charcoal*			405	65
S-862	Draper	House 2		Wood Charcoal*			430	85
S-863	Draper	House 2		Wood Charcoal*			495	65
S-861	Draper	House 2		Wood Charcoal*			570	95
S-818	Draper	House 2		Wood Charcoal*			590	75
UGAMS-22833	Draper	Sq 230-215 Midden 52 Level 4		*Zea mays*	-10.1	0.1	330	25
UGAMS-22834	Draper	S. Field Sq 940-160 House 33 Pit #1		Wood Charcoal*	-25.5	0.1	370	25
UGAMS-22835	Draper	Segment D expansion 2 Sq 290-185 House 7 Feature 11 Level 1		*Zea mays*	-9.4	0.1	270	25
VERA-6283	Draper	AlGt-2_9		*Zea mays*	-25.4	0.8	116	18
VERA-6283_2	Draper	AlGt-2_9		*Zea mays*	-12	0.9	306	29
VERA-6283_3	Draper	AlGt-2_9		*Zea mays*	-15.2	0.6	243	33
VERA-6284	Draper	AlGt-2_1		*Zea mays*	-10.9	1.0	323	34
VERA-6284_2	Draper	AlGt-2_1		*Zea mays*	-11.5	0.8	279	29
VERA-6285	Draper	AlGt-2_6		*Zea mays*	-11.2	0.8	323	28
VERA-6285_2	Draper	AlGt-2_6		*Zea mays*	-25.7	1.4	298	35
VERA-6285HS_2	Draper	AlGt-2_6		*Zea mays*	-9.1	0.7	292	26
VERA-6286	Draper	AlGt-2_7		*Zea mays*	-10.3	0.8	256	29
VERA-6286_2	Draper	AlGt-2_7		*Zea mays*	-10	0.7	302	26
VERA-6287	Draper	AlGt-2_2		*Zea mays*	-10.8	0.9	291	39
VERA-6287HS_2	Draper	AlGt-2_2		*Zea mays*	-8.9	0.8	298	28
UGA-22312	Spang	Sq 335-705 Midden 2 Level 4		*Zea mays*	-10.8	0.1	300	20
OxA-33077	Spang	335-705 SS25 Midden 2 Level 3		*Zea mays*	-11.07	0.3	371	25
VERA-6226	Spang	335-705 SS25 Midden 2 Level 3		*Zea mays*	-12	0.7	311	33
VERA-6226_2	Spang	335-705 SS25 Midden 2 Level 3		*Zea mays*	-9.4	1.0	324	33

VERA-6227	Spang	335-705 SS25 Midden 2 Level 3		*Zea mays*	-12.3	0.6	327	39
VERA-6227HS	Spang	335-705 SS25 Midden 2 Level 3		*Zea mays*	-11.1	0.9	266	39
VERA-6227_2	Spang	335-705 SS25 Midden 2 Level 3		*Zea mays*	-9.7	0.9	359	34
UGA-22311	Spang	Sq 335-705 Midden 2 Level 3		*Zea mays*	-9.9	0.1	270	20
Beta-217159	Mantle	365-130 Feature 253	Multiple	*Zea mays*	-7.6		370	40
GrM-13833	Mantle	159 435-180 Feature 427	Early	*Fragaria virginiana*	-25.59	0.12	373	15
GrM-13834	Mantle	159 435-180 Feature 427	Early	Wood Charcoal, *Fraxinus* sp.	-25.25	0.12	331	15
GrM-13835	Mantle	159 435-180 Feature 427	Early	Wood Charcoal, *Ulmus* sp.	-23.21	0.12	329	15
GrM-13837	Mantle	159 435-180 Feature 427	Early	Wood Charcoal, *Fagus* sp.	-24.61	0.12	320	15
GrM-13838	Mantle	91 535-190 Feature 718	Early	Wood Charcoal, *Fraxinus* sp.	-25.73	0.12	348	15
GrM-13839	Mantle	91 535-190 Feature 718	Early	Wood Charcoal, *Acer* sp.	-24.3	0.12	388	15
GrM-13840	Mantle	91 535-190 Feature 718	Early	Wood Charcoal, *Fagus* sp.	-25.45	0.12	338	15
GrM-13842	Mantle	144 415-155 Feature 648	Early	Wood Charcoal, *Acer* sp.	-24.01	0.15	469	15
GrM-13844	Mantle	144 415-155 Feature 648	Early	Wood Charcoal, *Fagus* sp.	-24.15	0.15	854	15
OxA-33078	Mantle	91 535-190 Feature 718	Early	*Zea mays*	-9.74	0.3	376	26
OxA-33079	Mantle	91 535-190 Feature 718	Early	*Zea mays*	-8.48	0.3	401	25
OxA-33080	Mantle	57 470-155 Feature 1005	Multiple	*Zea mays*	-8.90	0.3	356	25
OxA-33081	Mantle	40 450-120 Feature 1237	Late	*Zea mays*	-9.95	0.3	374	25
OxA-33082	Mantle	40 450-120 Feature 1237	Late	*Zea mays*	-8.68	0.3	414	25
OxA-33083	Mantle	21 495-165 Feature 934	Multiple	*Zea mays*	-10.00	0.3	423	25
UGAMS-22831	Mantle	House 20 Feature (support post)	Multiple	*Zea mays*	-8.7	0.1	330	25
UGAMS-22832	Mantle	Feature 709	Multiple	*Zea mays*	-9.2	0.1	360	25
VERA-6212	Mantle	144 4150155 Feature 648	Early	*Fragaria virginiana*	-26.6	0.7	353	37
VERA-6212_2	Mantle	144 415-155 Feature 648	Early	*Fragaria virginiana*	-28.9	1.2	368	38
VERA-6213	Mantle	91 535-190 Feature 718	Early	*Zea mays*	-8.9	0.7	349	32

VERA-6213_2	Mantle	91 535-190 Feature 718	Early	*Zea mays*	-7.9	1.0	335	35
VERA-6214	Mantle	159 435-180 Feature 427	Early	*Zea mays*	-8.5	0.5	357	36
VERA-6214_2	Mantle	159 435-180 Feature 427	Early	*Zea mays*	-6.5	1.1	351	34
VERA-6215	Mantle	166 400-200 Feature 492	Mid-Late	*Zea mays*	-8.6	0.8	370	38
VERA-6215HS	Mantle	166 400-200 Feature 492	Mid-Late	*Zea mays*	-5.7	0.6	333	34
VERA-6215_2	Mantle	166 400-200 Feature 492	Mid-Late	*Zea mays*	-8.9	1.2	281	34
VERA-6216	Mantle	126 530-165 Feature 709	Late	*Zea mays*	-11	0.8	316	34
VERA-6217	Mantle	36 465-125 Feature 1238	Very Late	*Zea mays*	-10.9	0.7	296	33
VERA-6217HS	Mantle	36 465-125 Feature 1238	Very Late	*Zea mays*	-10.1	0.7	344	33
VERA-6218	Mantle	164 370-185 Feature 238	Mid-Late/Late?	*Zea mays*	-8.2	0.7	342	36
VERA-6219	Mantle	40 450-120 Feature 1237	Late	*Zea mays*	-11.1	0.6	312	38
VERA-6220	Mantle	183 425-135 Feature 468	Late	*Zea mays*	-13.4	0.7	389	35
VERA-6220HS	Mantle	183 425-135 Feature 468	Late	*Zea mays*	-10	0.9	351	39
VERA-6221	Mantle	207 335-180 Feature 156	Very Late	*Zea mays*	-15.7	0.6	324	35
VERA-6222	Mantle	20 495-160 Feature 927B	Multiple, Earlier? = Earlier	*Fragaria virginiana*	-29.5	0.7	361	34
VERA-6223Cu	Mantle	21 495-165 Feature 934	Multiple	*Zea mays*	-12	0.6	369	37
VERA-6223	Mantle	21 495-165 Feature 934	Multiple	*Zea mays*	-13.5	0.8	318	35
VERA-6223HS	Mantle	21 495-165 Feature 934	Multiple	*Zea mays*	-10.2	0.7	326	38
VERA-6224Cu	Mantle	57 470-155 Feature 1005	Multiple	*Zea mays*	-10.4	0.8	373	36
VERA-6224	Mantle	57 470-155 Feature 1005	Multiple	*Zea mays*	-12.1	0.7	326	37
VERA-6225HS	Mantle	20 495-160 Feature 927B	Multiple, Earlier? = Earlier	*Fragaria virginiana*	-29.7	0.7	408	33
UGAMS-25450	Warminster	Feature 16B		*Phaseolus* sp.	-24.6	0.1	363	22
UGAMS-25451	Warminster	Feature 12		*Prunus americana*	-27.2	0.1	427	22
UGAMS-25451-u	Warminster	Feature 12		*Prunus americana*	-27.6	0.1	365	21
UGAMS-25451-r2	Warminster	Feature 12		*Prunus americana*	-27.3	0.1	355	22
UGAMS-25451-r2r	Warminster	Feature 12		*Prunus americana*	-27.8	0.1	368	21
UGAMS-25451-r	Warminster	Feature 12		*Prunus americana*	-27.1	0.1	396	21
UGAMS-25451-rr	Warminster	Feature 12		*Prunus americana*	-28.0	0.1	346	21
UGAMS-34181	Warminster	H9 Feature 30c		*Zea mays*	-9.5	0.1	365	21
UGAMS-34182	Warminster	H5 Feature 1		*Zea mays*	-10.9	0.1	326	21
VERA-6309_1	Warminster	Feature 16B		*Phaseolus* sp.	-22.7	0.8	314	28
VERA-6309_2	Warminster	Feature 16B		*Phaseolus* sp.	-24.7	1.1	311	28
VERA-6309_3	Warminster	Feature 16B		*Phaseolus* sp.	-26.8	0.6	374	40
VERA-6310	Warminster	Feature 12		*Prunus americana*	-27.6	0.9	334	28
VERA-6310_2	Warminster	Feature 12		*Prunus americana*	27.0	0.7	340	31
Wk-42865	Warminster	Feature 13, Rings 9-17		*Larix laricina*			355	17

Wk-42866	Warminster	Feature 13, Rings 19-27		*Larix laricina*			325	15
Wk-42867	Warminster	Feature 13, Rings 29-37		*Larix laricina*			349	13
Wk-42868	Warminster	Feature 13, Rings 39-47		*Larix laricina*			321	15
Wk-42869	Warminster	Feature 13, Rings 49-57		*Larix laricina*			317	14

Table S2. UGAMS radiocarbon dates on the Warminster Feature 12 *Prunus Americana* (plum) sample using several different pretreatment approaches (data as listed in table S1). The approaches employed for each iteration of the analysis are detailed below for each of the (sub-) samples. This process occurred as the original date, UGAMS-25451, appeared to be somewhat older than the other dates from House 4 at Warminster and so was considered as perhaps an outlier, and we wished to better assess the likely appropriate radiocarbon age of this sample for this study. The outcome is assessed below.

UGAMS Date	Sample	^{14}C Age BP	SD
UGAMS-25451	Feature 12, *Prunus americana*	427	22
Standard UGAMS AAA pretreatment, then sample combusted at 900°C in an evacuated and sealed quartz tube in the presence of CuO to produce CO_2 which was then dated by the AMS (84).			
UGAMS-25451-u	Feature 12, *Prunus americana*	365	21
No pretreatment. Sample combusted at 900°C in an evacuated and sealed quartz tube in the presence of CuO to produce CO_2 which was then dated by the AMS.			
UGAMS-25451-r2	Feature 12, *Prunus americana*	355	22
Complete re-analysis starting with untreated sample following Standard UGAMS AAA pretreatment, then sample combusted at 900°C in an evacuated and sealed quartz tube in the presence of CuO to produce CO_2 which was then dated by the AMS (84). Note: this re-analysis date is significantly different (more than 2SD) from the original date (a chi-squared test shows the two dates are not compatible at the 95% level with being the same radiocarbon age: χ^2 df1, T=5.4 > 3.8 (97)).			
UGAMS-25451-r2r	Feature 12, *Prunus americana*	368	21
Remnants of UGAMS-25451-r2 were subjected to a second AAA pretreatment and then usual combustion at 900°C in an evacuated and sealed quartz tube in the presence of CuO to produce CO_2 which was then dated by the AMS (84).			
UGAMS-25451-r	Feature 12, *Prunus americana*	396	21
A remnant of the original pretreated sample (as used for UGAMS-25451) was combusted without additional pretreatment at 900°C in an evacuated and sealed quartz tube in the presence of CuO to produce CO_2 which was then dated by the AMS (84).			
UGAMS-25451-rr	Feature 12, *Prunus americana*	346	21
A remnant of the original pretreated sample (as used for UGAMS-25451) was subjected to a second AAA pretreatment and then combusted at 900°C in an evacuated and sealed quartz tube in the presence of CuO to produce CO_2 which was then dated by the AMS (84).			

Overall assessment:

While the original date, UGAMS-25451, is the oldest age in the set of six measurements on the same sample, all six data may be regarded as plausible estimates of the same real ^{14}C age (weighted average 376±9 ^{14}C years BP) within 95% probability limits: χ^2 df5, T=9.7 < 11.1 (*97*). There is no *a priori* reason therefore to exclude UGAMS-25451.

Table S3. Details of the results from the Mantle internal site sequence model in fig. S9.

Element	68.2% hpd	95.4% hpd
Start Mantle	1598-1613	1466-1517 (9.5%) 1576-1618 (85.9%)
Date Mantle Early	1601-1615	1492-1543 (8.9%) 1573-1621 (86.5%)
Span Mantle Early (years)	*0-7*	*0-40 (93.4%)* *59-84 (2.0%)*
Early/Earlier to Mid-Late Transition	1603-1616	1505-1522 (4.4%) 1552-1624 (91.4%)
Date Mantle Mid-Late	1605-1618	1506-1520 (3.1%) 1561-1628 (92.3%)
Span Mantle Mid-Late (years)	*0-3*	*0-15*
Mid-Late to Late Transition	1605-1620	1508-1521 (2.9%) 1579-1631 (92.5%)
Date Mantle Late	1608-1622	1510-1523 (2.6%) 1590-1634 (92.4%)
Span Mantle Late (years)	*0-5*	*0-17*
Late to Very Late Transition	1610-1625	1513-1523 (2.1%) 1596-1638 (93.3%)
Date Mantle Very Late	1612-1632	1513-1527 (2.2%) 1595-1653 (93.2%)
Span Mantle Very Late (years)	*0-5*	*0-19*
End Mantle	1613-1638	1513-1531 (2.2%) 1595-1669 (93.2%)

Table S4. Order calculation from OxCal determining the probability that t_1 is less than (i.e., older than) t_2. The three site Phases for the Draper, Spang, and Mantle sites (all data as in fig. S2) were placed within a parent Phase, and the Order function was used to calculate the relative probabilities for the order of the site Phases within this parent Phase. We compared the Order probabilities for the Date PDFs for the Draper, Spang, and Mantle Phases.

$t_1 < t_2$	t_2 Draper	t_2 Spang	t_2 Mantle
t_1 Draper	0	0.5609	0.6712
t_1 Spang	0.4391	0	0.6279
t_1 Mantle	0.3288	0.3721	0

Table S5. OxCal runfiles for the Warminster site in Fig. 2. Table S5A is the OxCal runfile for Figs. 2A and 2B, table S5B is the OxCal runfile for Fig. 2C. As discussed in the Supplementary Material above, in table S5A the ^{14}C dates on the same plum and bean samples are combined, whereas, in table S5B, each of the dates on the plum and on the bean samples are instead treated separately within independent 'plum' and 'bean' Phases (so each date as a member of a group of events that are assumed to be randomly sampled from a uniform distribution) within the overall Phase of short-lived plant material from Warminster. In the run for Fig. 2D the UGAMS-25451 sample was excluded (the relevant lines of code are marked with yellow highlight in table S5B).

Table S5A:

```
Options()
 {
  Resolution=1;
 };
 Plot()
 {
  Outlier_Model("General",T(5),U(0,4),"t");
  Outlier_Model("SSimple",N(0,2),0,"s");
  D_Sequence("WAR-1 Larix laricina")
  {
   First ();
   R_Date ("Wk-42865 Rings 9-17",355,17)
   {
    Outlier ("SSimple",0.05);
   };
   Gap(10);
   R_Date ("Wk-42866 Rings 19-27",325,15)
   {
    Outlier ("SSimple",0.05);
   };
   Gap(10);
   R_Date ("Wk-42867 Rings 29-37",349,13)
```

```
 {
  Outlier ("SSimple",0.05);
 };
 Gap(10);
 R_Date ("Wk-42868 Rings 39-47",321,15)
 {
  Outlier ("SSimple",0.05);
 };
 Gap(10);
 R_Date ("Wk-42869 Rings 49-57",317,14)
 {
  Outlier ("SSimple",0.05);
 };
 Gap(4);
 Date ("RY57 last extant ring");
};
Sequence ("Warminster")
{
 Boundary ("Start Warminster");
 After( "WAR-1 Last Extant Ring TPQ")
 {
  Date("=RY57 last extant ring");
 };
 Phase ("Warminster Short-Lived Samples")
 {
  R_Combine ("Warminster H4 F12 plum (Prunus Americana)",8)
  {
   Outlier("General", 0.05);
   R_Date ("VERA-6310 H4 F12 plum",334,28)
   {
    Outlier("SSimple", 0.05);
   };
   R_Date ("VERA-6310_2 H4 F12 plum",340,31)
   {
    Outlier("SSimple", 0.05);
```

```
};
R_Date ("UGAMS-25451 F12 plum",427,22)
{
 Outlier("SSimple", 0.05);
};
R_Date ("UGAMS-25451-u F12 plum",365,21)
{
 Outlier("SSimple", 0.05);
};
R_Date ("UGAMS-25451-r2 F12 plum",355,22)
{
 Outlier("SSimple", 0.05);
};
R_Date ("UGAMS-25451-r2r F12 plum",368,21)
{
 Outlier("SSimple", 0.05);
};
R_Date ("UGAMS-25451-r F12 plum",396,21)
{
 Outlier("SSimple", 0.05);
};
R_Date ("UGAMS-25451-rr F12 plum",346,21)
{
 Outlier("SSimple", 0.05);
};
};
R_Combine ("Warminster H4 F16B bean (Phaseolus)",8)
{
 Outlier("General", 0.05);
 R_Date ("VERA-6309_1 H4 F16B bean",314,28)
 {
  Outlier("SSimple", 0.05);
 };
 R_Date ("VERA-6309_2 H4 F16B bean",311,28)
 {
```

```
    Outlier("SSimple", 0.05);
   };
   R_Date ("VERA-6309_3 H4 F16B bean",374,40)
   {
    Outlier("SSimple", 0.05);
   };
   R_Date ("UGAMS-25450 H4 F16 bean",363,22)
   {
    Outlier("SSimple", 0.05);
   };
  };
  R_Date ("Warminster_4_UGAMS34181 maize H9, F30c",365,21)
  {
   Outlier ("General",0.05);
  };
  R_Date ("Warminster_8_UGAMS34182 maize H5, F1",326,21)
  {
   Outlier ("General",0.05);
  };
  Date ("Warminster Date Estimate");
 };
 Boundary ("End Warminster");
};
C_Date("Champlain at Cahiagué in 1615 CE",1615);
C_Date("Champlain at Cahiagué in 1616 CE",1616);
};
```

Table S5B:

```
Options()
{
 Resolution=1;
};
Plot()
```

```
{
 Outlier_Model("General",T(5),U(0,4),"t");
 Outlier_Model("SSimple",N(0,2),0,"s");
 D_Sequence("WAR-1 Larix laricina")
 {
  First ();
  R_Date ("Wk-42865 Rings 9-17",355,17)
  {
   Outlier ("SSimple",0.05);
  };
  Gap(10);
  R_Date ("Wk-42866 Rings 19-27",325,15)
  {
   Outlier ("SSimple",0.05);
  };
  Gap(10);
  R_Date ("Wk-42867 Rings 29-37",349,13)
  {
   Outlier ("SSimple",0.05);
  };
  Gap(10);
  R_Date ("Wk-42868 Rings 39-47",321,15)
  {
   Outlier ("SSimple",0.05);
  };
  Gap(10);
  R_Date ("Wk-42869 Rings 49-57",317,14)
  {
   Outlier ("SSimple",0.05);
  };
  Gap(4);
  Date ("RY57 last extant ring");
 };
 Sequence ("Warminster")
 {
```

```
Boundary ("Start Warminster");
After( "WAR-1 Last Extant Ring TPQ")
{
 Date("=RY57 last extant ring");
};
Phase ("Warminster Short-Lived Samples")
{
 Sequence ("Warminster H4 F12 plum (Prunus americana)")
 {
  Boundary ("Start Plum");
  Phase ("Plum")
  {
   R_Date ("VERA-6310 H4 F12 plum",334,28)
   {
    Outlier ("General",0.05);
   };
   R_Date ("VERA-6310_2 H4 F12 plum",340,31)
   {
    Outlier ("General",0.05);
   };
   R_Date ("UGAMS-25451 H4 F12 plum",427,22)
   {
    Outlier ("General",0.05);
   };
   R_Date ("UGAMS-25451-u H4 F12 plum",365,21)
   {
    Outlier ("General",0.05);
   };
   R_Date ("UGAMS-25451-r2 H4 F12 plum",355,22)
   {
    Outlier ("General",0.05);
   };
   R_Date ("UGAMS-25451-r2r H4 F12 plum",368,21)
   {
    Outlier ("General",0.05);
```

```
 };
 R_Date ("UGAMS-25451-r H4 F12 plum",396,21)
 {
  Outlier ("General",0.05);
 };
 R_Date ("UGAMS-25451-rr H4 F12 plum",346,21)
 {
  Outlier ("General",0.05);
 };
};
 Boundary ("End Plum");
};
Sequence ("Warminster H4 F16B bean (Phaseolus)")
{
 Boundary ("Start Bean");
 Phase ("Bean")
 {
  R_Date ("VERA-6309_1 H4 F16B bean",314,28)
  {
   Outlier ("General",0.05);
  };
  R_Date ("VERA-6309_2 H4 F16B bean",311,28)
  {
   Outlier ("General",0.05);
  };
  R_Date ("VERA-6309_3 H4 F16B bean",374,40)
  {
   Outlier ("General",0.05);
  };
  R_Date ("UGAMS-25450 H4 F16B bean",363,22)
  {
   Outlier ("General",0.05);
  };
 };
 Boundary ("End Bean");
```

```
  };
  R_Date ("Warminster_4_UGAMS34181 maize H9, F30c",365,21)
  {
   Outlier ("General",0.05);
  };
  R_Date ("Warminster_8_UGAMS34182 maize H5, F1",326,21)
  {
   Outlier ("General",0.05);
  };
  Date ("Warminster Date Estimate");
  Span ("Span Warminster");
 };
 Boundary ("End Warminster");
};
C_Date("Champlain at Cahiagué in 1615 CE",1615);
C_Date("Champlain at Cahiagué in 1616 CE",1616);
};
```

Table S6. OxCal runfile for the Draper, Spang, and Mantle site analysis shown in Fig. 3. The analysis of the three sites (their respective Phases) is independent of each other. The six samples indicated by yellow highlight are found there to be minor possible outliers within their R_Combines. The results from a re-run of the model excluding these 6 dates are reported in fig. S7. "IA" = Inbuilt Age is the Charcoal Outlier model of ref. 37.

```
Options()
 {
  Resolution=1;
 };
 Plot()
 {
  Outlier_Model("SSimple",N(0,2),0,"s");
  Outlier_Model("General",T(5),U(0,4),"t");
  Outlier_Model("IA",Exp(1,-10,0),U(0,3),"t");
  Sequence ()
  {
   Boundary ("Start Draper");
   Phase ("Draper")
   {
    R_Date("S-819 Charcoal House 2",210,80)
    {
     Outlier("IA", 1);
    };
    R_Date("S-860 Charcoal House 2",405,65)
    {
     Outlier("IA", 1);
    };
    R_Date("S-862 Charcoal House 2",430,85)
    {
     Outlier("IA", 1);
    };
    R_Date("S-863 Charcoal House 2",495,65)
    {
```

```
 Outlier("IA", 1);
};
R_Date("S-861 Charcoal House 2",570,95)
{
 Outlier("IA", 1);
};
R_Date("S-818 Charcoal House 2",590,75)
{
 Outlier("IA", 1);
};
R_Date("UGAMS-22833 maize; Sq230-215, Midden 52, level 4",330,25)
{
 Outlier ("General",0.05);
};
R_Date("UGAMS-22834 charcoal S field; Sq940-160; H33, Pit #1",370,25)
{
 Outlier("IA", 1);
};
R_Date("UGAMS-22835 maize; exp 2; Sq290-185; H7, F11, level 1",270,25)
{
 Outlier ("General",0.05);
};
R_Date("VERA-6283_2 maize Draper_AlGt-2_9",306,29)
{
 Outlier ("General",0.05);
};
R_Combine ("AlGt-2_1 maize",8)
{
 Outlier ("General",0.05);
 R_Date("VERA-6284 maize Draper_AlGt-2_1",323,34)
 {
  Outlier("SSimple",0.05);
 };
 R_Date("VERA-6284_2 maize Draper_AlGt-2_1",279,29)
 {
```

```
 Outlier("SSimple",0.05);
 };
};
R_Combine ("AlGt-2_6 maize",8)
{
 Outlier ("General",0.05);
 R_Date("VERA-6285 maize Draper_AlGt-2_6",323,28)
 {
  Outlier("SSimple",0.05);
 };
 R_Date("VERA-6285HS_2 maize Draper_AlGt-2_6",292,26)
 {
  Outlier("SSimple",0.05);
 };
};
R_Combine ("AlGt-2_7 maize",8)
{
 Outlier ("General",0.05);
 R_Date("VERA-6286 maize Draper_AlGt-2_7",256,29)
 {
  Outlier("SSimple",0.05);
 };
 R_Date("VERA-6286_2 maize Draper_AlGt-2_7",302,26)
 {
  Outlier("SSimple",0.05);
 };
};
R_Combine ("AlGt-2_2 maize",8)
{
 Outlier ("General",0.05);
 R_Date("VERA-6287 maize Draper_AlGt-2_2",291,39)
 {
  Outlier("SSimple",0.05);
 };
 R_Date("VERA-6287HS_2 maize Draper_AlGt-2_2",298,28)
```

```
  {
   Outlier("SSimple",0.05);
  };
 };
 Date ("Date Draper");
 Span ("Span Draper");
};
Boundary ("End Draper");
};
Sequence ()
{
 Boundary ("Start Spang");
 Phase (“Spang”)
 {
  R_Date("AlGt-66 UGA-22312 maize Sq. 335-705; Midden 2, level 4",300,20)
  {
   Outlier ("General",0.05);
  };
  R_Date("VERA-6227 maize 335-705 SS25 Midden 2 Level 3",327, 39)
  {
   Outlier ("General",0.05);
  };
  R_Date("VERA-6227HS maize 335-705 SS25 Midden 2 Level 3",266,39)
  {
   Outlier ("General",0.05);
  };
  R_Date("VERA-6227_2 maize 335-705 SS25 Midden 2 Level 3",359,34)
  {
   Outlier ("General",0.05);
  };
  R_Date ("OxA-33077 maize 335-705 Midden 2 Level 3", 371,25)
  {
   Outlier ("General",0.05);
  };
  R_Date("VERA-6226 maize 335-705 SS25 Midden 2 Level 3",311,33)
```

```
  {
   Outlier ("General",0.05);
  };
  R_Date("VERA-6226_2 maize 335-705 SS25 Midden 2 Level 3",324,33)
  {
   Outlier ("General",0.05);
  };
  R_Date("AlGt-66 maize UGA-22311 Sq. 335-705; Midden 2, level 3",270,20)
  {
   Outlier ("General",0.05);
  };
 Date ("Date Spang");
 Span ("Span Spang ");
};
Boundary ("End Spang");
};
Sequence ()
{
 Boundary ("Start Mantle");
 Phase ("Mantle")
 {
  R_Date("GrM-13842 144 415-155 F648 Charcoal",469,15)
  {
   Outlier ("IA",1);
  };
  R_Date("GrM-13844 144 415-155 F648 Charcoal",854,15)
  {
   Outlier ("IA",1);
  };
  R_Combine ("144 415-155 Feature 648 strawberry seeds",8)
  {
   Outlier ("General",0.05);
   R_Date("VERA-6212 144 415-155 F648 strawberry seeds",353,37)
   {
    Outlier ("SSimple",0.05);
```

```
 };
 R_Date("VERA-6212_2 144 415-155 F648 strawberry seeds",368,38)
 {
  Outlier ("SSimple",0.05);
 };
};
R_Date("GrM-13838 91 535-190 F718 Charcoal",348,15)
{
 Outlier("IA",1);
};
R_Date("GrM-13839 91 535-190 F718 Charcoal",388,15)
{
 Outlier("IA",1);
};
R_Date("GrM-13840 91 535-190 F718 Charcoal",338,15)
{
 Outlier("IA",1);
};
R_Combine ("91 535-190 F718 Maize",8)
{
 Outlier("General",0.05);
 R_Date("VERA-6213 91 535-190 F718 Maize",349,32)
 {
  Outlier ("SSimple",0.05);
 };
 R_Date("VERA-6213_2 91 535-190 F718 Maize",335,35)
 {
  Outlier ("SSimple",0.05);
 };
 R_Date("OxA-33078 91 535-190 F718 Maize",376,26)
 {
  Outlier ("SSimple",0.05);
 };
 R_Date("OxA-33079 91 535-190 F718 Maize",401,25)
 {
```

```
   Outlier ("SSimple",0.05);
  };
 };
 R_Date("GrM-13834 159 435-180 F427 Charcoal",331,15)
 {
  Outlier("IA",1);
 };
 R_Date("GrM-13835 159 435-180 F427 Charcoal",329,15)
 {
  Outlier("IA",1);
 };
 R_Date("GrM-13837 159 435-180 F427 Charcoal",320,15)
 {
  Outlier("IA",1);
 };
 R_Combine ("159 435-180 F427 Maize",8)
 {
  Outlier ("General",0.05);
  R_Date("VERA-6214 159 435-180 F427 Maize",357,36)
  {
   Outlier("SSimple",0.05);
  };
  R_Date("VERA-6214_2 159 435-180 F427 Maize",351,34)
  {
   Outlier("SSimple",0.05);
  };
 };
 R_Date("GrM-13833 159 435-180 F427 Strawberry seeds",373,15)
 {
  Outlier("General",0.05);
 };
 R_Date("VERA-6222 20 495-160 F927B Strawberry seeds",361,34)
 {
  Outlier ("General",0.05);
 };
```

```
R_Date("VERA-6225HS 20 495-160 F927B Strawberry seeds",408,33)
{
 Outlier ("General",0.05);
};
R_Combine ("166 400-200 F492 Maize",8)
{
 Outlier ("General",0.05);
 R_Date("VERA-6215 166 400-200 F492 Maize",370,38)
 {
  Outlier("SSimple",0.05);
 };
 R_Date("VERA-6215HS 166 400-200 F492 Maize",333,34)
 {
  Outlier("SSimple",0.05);
 };
 R_Date("VERA-6215_2 166 400-200 F492 Maize",281,34)
 {
  Outlier("SSimple",0.05);
 };
};
R_Date("VERA-6218 164 370-185 F238 Maize",342,36)
{
 Outlier ("General",0.05);
};
R_Date("VERA-6216 126 530-165 F709 Maize",316,34)
{
 Outlier ("General",0.05);
};
R_Combine ("40 450-120 F1237 Maize",8)
{
 Outlier ("General",0.05);
 R_Date("VERA-6219 40 450-120 F1237 Maize",312,38)
 {
  Outlier("SSimple",0.05);
 };
```

```
 R_Date("OxA-33081 40 450-120 F1237 Maize",374,25)
 {
  Outlier("SSimple",0.05);
 };
 R_Date("OxA-33082 40 450-120 F1237 Maize",414,25)
 {
  Outlier("SSimple",0.05);
 };
};
R_Combine ("183 425-135 F468 Maize",8)
{
 Outlier("General",0.05);
 R_Date("VERA-6220 183 425-135 F468 Maize",389,35)
 {
  Outlier("SSimple",0.05);
 };
 R_Date("VERA-6220HS 183 425-135 F468 Maize",351,39)
 {
  Outlier("SSimple",0.05);
 };
};
R_Combine ("36 465-125 F1238 Maize",8)
{
 Outlier("General",0.05);
 R_Date("VERA-6217 36 465-125 F1238 Maize",296,33)
 {
  Outlier("SSimple",0.05);
 };
 R_Date("VERA-6217HS 36 465-125 F1238 Maize",344,33)
 {
  Outlier("SSimple",0.05);
 };
};
Date ("Date Mantle");
Span ("Span Mantle");
```

```
  };
  Boundary ("End Mantle");
 };
};
```

Table S7. OxCal runfile for the Spang Sequence analysis shown in fig. S8.

```
Options()
 {
  Resolution=1;
 };
 Plot()
 {
  Outlier_Model("General",T(5),U(0,4),"t");
  Sequence ("Spang")
  {
   Boundary ("Start Spang");
   Phase (“Spang Midden 2 Level 4”)
   {
    R_Date("AlGt-66 UGA-22312 maize cob Sq. 335-705; Midden 2, level 4",300,20)
    {
     Outlier ("General",0.05);
    };
   };
   Boundary ("Transition Level 4 to Level 3");
   Phase ("Spang Midden 2 Level 3")
   {
    R_Date("VERA-6227 335-705 SS25 Midden 2 Level 3 Maize",327, 39)
    {
     Outlier ("General",0.05);
    };
    R_Date("VERA-6227HS 335-705 SS25 Midden 2 Level 3 Maize",266,39)
    {
     Outlier ("General",0.05);
    };
    R_Date("VERA-6227_2 335-705 SS25 Midden 2 Level 3 Maize",359,34)
    {
     Outlier ("General",0.05);
    };
    R_Date ("OxA-33077 335-705 Midden 2 Level 3 Maize", 371,25)
```

```
  {
   Outlier ("General",0.05);
  };
  R_Date("VERA-6226 335-705 SS25 Midden 2 Level 3 Maize",311, 33)
  {
   Outlier ("General",0.05);
  };
  R_Date("VERA-6226_2 335-705 SS25 Midden 2 Level 3 Maize",324, 33)
  {
   Outlier ("General",0.05);
  };
  R_Date("AlGt-66 UGA-22311 maize Sq. 335-705; Midden 2, level 3",270,20)
  {
   Outlier ("General",0.05);
  };
  Date ("Date Spang Midden 2 Level 3");
  Span ("Span Spang Midden 2 Level 3");
 };
 Boundary ("End Spang");
};
```

Table S8. OxCal runfile for the Mantle Sequence analysis shown in fig. S9 and with results in table S3. "IA" = Inbuilt Age is the Charcoal Outlier model of ref. 35.

```
Options()
 {
  Resolution=1;
 };
 Plot()
 {
  Outlier_Model("General",T(5),U(0,4),"t");
  Outlier_Model("SSimple",N(0,2),0,"s");
  Outlier_Model("IA",Exp(1,-10,0),U(0,3),"t");
  Sequence ("Mantle Secure Site Sequence")
  {
   Boundary ("Start Mantle");
   Phase ("Mantle EARLY")
   {
    R_Date("GrM-13842 144 415-155 Feature 648 Charcoal",469,15)
    {
     Outlier ("IA",1);
    };
    R_Date("GrM-13844 144 415-155 Feature 648 Charcoal",854,15)
    {
     Outlier ("IA",1);
    };
    R_Combine ("Mantle 144 415-155 Feature 648 strawberry seeds, EARLY")
    {
     Outlier ("General",0.05);
     R_Date("VERA-6212 144 415-155 Feature 648 strawberry seeds, EARLY",353,37)
     {
      Outlier ("SSimple",0.05);
     };
     R_Date("VERA-6212_2 144 415-155 Feature 648 strawberry seeds, EARLY",368,38)
     {
```

```
 Outlier ("SSimple",0.05);
 };
};
R_Date("GrM-13838 91 535-190 Feature 718 Charcoal",348,15)
{
 Outlier("IA",1);
};
R_Date("GrM-13839 91 535-190 Feature 718 Charcoal",388,15)
{
 Outlier("IA",1);
};
R_Date("GrM-13840 91 535-190 Feature 718 Charcoal",338,15)
{
 Outlier("IA",1);
};
R_Combine ("Mantle 91 535-190 Feature 718 Maize, EARLY")
{
 Outlier("General",0.05);
 R_Date("VERA-6213 91 535-190 Feature 718 Maize, EARLY",349,32)
 {
  Outlier ("SSimple",0.05);
 };
 R_Date("VERA-6213_2 91 535-190 Feature 718 Maize, EARLY",335,35)
 {
  Outlier ("SSimple",0.05);
 };
 R_Date("OxA-33078 91 535-190 Feature 718 Maize, EARLY",376,26)
 {
  Outlier ("SSimple",0.05);
 };
 R_Date("OxA-33079 91 535-190 Feature 718 Maize, EARLY",401,25)
 {
  Outlier ("SSimple",0.05);
 };
};
```

```
 R_Date("GrM-13834 159 435-180 Feature 427 Charcoal",331,15)
 {
  Outlier("IA",1);
 };
 R_Date("GrM-13835 159 435-180 Feature 427 Charcoal",329,15)
 {
  Outlier("IA",1);
 };
 R_Date("GrM-13837 159 435-180 Feature 427 Charcoal",320,15)
 {
  Outlier("IA",1);
 };
 R_Combine ("Mantle 159 435-180 Feature 427 Maize")
 {
  Outlier ("General",0.05);
  R_Date("VERA-6214 159 435-180 Feature 427 Maize, EARLY",357,36)
  {
   Outlier("SSimple",0.05);
  };
  R_Date("VERA-6214_2 159 435-180 Feature 427 Maize, EARLY",351,34)
  {
   Outlier("SSimple",0.05);
  };
  R_Date("GrM-13833 159 435-180 Feature 427 Maize, EARLY",373,15)
  {
   Outlier("SSimple",0.05);
  };
 };
 Date ("Date Mantle EARLY");
 Span ("Span Mantle EARLY");
};
Boundary ("EARLY/EARLIER to MID-LATE TRANSITION");
Phase ("Mantle MID-LATE")
{
 R_Combine ("Mantle 166 400-200 Feature 492 Maize, MID-LATE")
```

```
 {
  Outlier ("General",0.05);
  R_Date("VERA-6215 166 400-200 Feature 492 Maize, MID-LATE",370,38)
  {
   Outlier("SSimple",0.05);
  };
  R_Date("VERA-6215HS 166 400-200 Feature 492 humic acids from 1st subsample Maize, MID-LATE",333,34)
  {
   Outlier("SSimple",0.05);
  };
  R_Date("VERA-6215_2 166 400-200 Feature 492 Maize, MID-LATE",281,34)
  {
   Outlier("SSimple",0.05);
  };
 };
 R_Date("VERA-6218 164 370-185 Feature 238 Maize, MID-LATE/LATE?",342,36)
 {
  Outlier ("General",0.05);
 };
 Date ("Date Mantle MID-LATE");
 Span ("Span Mantle MID-LATE");
};
Boundary ("MID-LATE to LATE TRANSITION");
Phase ("Mantle LATE")
{
 R_Date("VERA-6216 126 530-165 Feature 709 Maize, LATE",316,34)
 {
  Outlier ("General",0.05);
 };
 R_Combine ("Mantle 40 450-120 Feature 1237 Maize, LATE")
 {
  Outlier ("General",0.05);
  R_Date("VERA-6219 40 450-120 Feature 1237 Maize, LATE",312,38)
  {
   Outlier("SSimple",0.05);
```

```
 };
 R_Date("OxA-33081 40 450-120 Feature 1237 Maize, LATE",374,25)
 {
  Outlier("SSimple",0.05);
 };
 R_Date("OxA-33082 40 450-120 Feature 1237 Maize, LATE",414,25)
 {
  Outlier("SSimple",0.05);
 };
};
R_Combine ("Mantle 183 425-135 Feature 468 Maize, LATE")
{
 Outlier("General",0.05);
 R_Date("VERA-6220 183 425-135 Feature 468 Maize, LATE",389,35)
 {
  Outlier("SSimple",0.05);
 };
 R_Date("VERA-6220HS 183 425-135 Feature 468 Maize, LATE",351,39)
 {
  Outlier("SSimple",0.05);
 };
};
Date ("Date Mantle LATE");
Span("Span Mantle LATE");
};
Boundary ("LATE to VERY LATE TRANSITION");
Phase ("Mantle VERY LATE")
{
 R_Date("VERA-6221 207 335-180 Feature 156 Maize, VERY LATE",324,35)
 {
  Outlier ("General",0.05);
 };
 R_Combine ("Mantle 36 465-125 Feature 1238 Maize, VERY LATE")
 {
  Outlier("General",0.05);
```

```
   R_Date("VERA-6217 36 465-125 Feature 1238 Maize, VERY LATE",296,33)
   {
    Outlier("SSimple",0.05);
   };
   R_Date("VERA-6217HS 36 465-125 Feature 1238 Maize, VERY LATE",344,33)
   {
    Outlier("SSimple",0.05);
   };
  };
  Date ("Date Mantle VERY LATE");
  Span ("Span Mantle VERY LATE");
 };
 Boundary ("End Mantle");
};
};
```

Table S9. The OxCal runfile for the Draper-Spang-Mantle sequence analysis shown in Fig. 4 and with results in Table 2. "IA" = Inbuilt Age is the Charcoal Outlier model of ref. 35.

```
Options()
 {
  Resolution=1;
 };
 Plot()
 {
  Outlier_Model("SSimple",N(0,2),0,"s");
  Outlier_Model("General",T(5),U(0,4),"t");
  Outlier_Model("IA",Exp(1,-10,0),U(0,3),"t");
  Sequence ("Draper-Spang-Mantle")
  {
   Boundary ("Start Draper");
   Phase ("Draper")
   {
    R_Date("S-819 Charcoal House 2",210,80)
    {
     Outlier("IA", 1);
    };
    R_Date("S-860 Charcoal House 2",405,65)
    {
     Outlier("IA", 1);
    };
    R_Date("S-862 Charcoal House 2",430,85)
    {
     Outlier("IA", 1);
    };
    R_Date("S-863 Charcoal House 2",495,65)
    {
     Outlier("IA", 1);
    };
    R_Date("S-861 Charcoal House 2",570,95)
    {
```

```
 Outlier("IA", 1);
};
R_Date("S-818 Charcoal House 2",590,75)
{
 Outlier("IA", 1);
};
R_Date("UGAMS-22833 maize; Sq230-215, Midden 52, level 4",330,25)
{
 Outlier ("General",0.05);
};
R_Date("UGAMS-22834 charcoal S field; Sq940-160; H33, Pit #1",370,25)
{
 Outlier("IA", 1);
};
R_Date("UGAMS-22835 maize; exp 2; Sq290-185; H7, F11, level 1",270,25)
{
 Outlier ("General",0.05);
};
R_Date("VERA-6283_2 maize Draper_AlGt-2_9",306,29)
{
 Outlier ("General",0.05);
};
R_Combine ("AlGt-2_1 maize",8)
{
 Outlier ("General",0.05);
 R_Date("VERA-6284 maize Draper_AlGt-2_1",323,34)
 {
  Outlier("SSimple",0.05);
 };
 R_Date("VERA-6284_2 maize Draper_AlGt-2_1",279,29)
 {
  Outlier("SSimple",0.05);
 };
};
R_Combine ("AlGt-2_6 maize",8)
```

```
{
 Outlier ("General",0.05);
 R_Date("VERA-6285 maize Draper_AlGt-2_6",323,28)
 {
  Outlier("SSimple",0.05);
 };
 R_Date("VERA-6285HS_2 maize Draper_AlGt-2_6",292,26)
 {
  Outlier("SSimple",0.05);
 };
};
R_Combine ("AlGt-2_7 maize",8)
{
 Outlier ("General",0.05);
 R_Date("VERA-6286 maize Draper_AlGt-2_7",256,29)
 {
  Outlier("SSimple",0.05);
 };
 R_Date("VERA-6286_2 maize Draper_AlGt-2_7",302,26)
 {
  Outlier("SSimple",0.05);
 };
};
R_Combine ("AlGt-2_2 maize",8)
{
 Outlier ("General",0.05);
 R_Date("VERA-6287 maize Draper_AlGt-2_2",291,39)
 {
  Outlier("SSimple",0.05);
 };
 R_Date("VERA-6287HS_2 maize Draper_AlGt-2_2",298,28)
 {
  Outlier("SSimple",0.05);
 };
};
```

```
 Date ("Date Draper");
 Span ("Span Draper");
};
Boundary("Mid End Draper")
{
 Transition("Duration End Draper");
 Start("Start End Draper");
 End("End End Draper");
};
Boundary("Mid Start Spang")
{
 Transition("Duration Start Spang");
 Start("Start Start Spang");
 End("End Start Spang");
};
Phase (“Spang”)
{
 R_Date("AlGt-66 UGA-22312 maize Sq. 335-705; Midden 2, level 4",300,20)
 {
  Outlier ("General",0.05);
 };
 R_Date("VERA-6227 maize 335-705 SS25 Midden 2 Level 3",327, 39)
 {
  Outlier ("General",0.05);
 };
 R_Date("VERA-6227HS maize 335-705 SS25 Midden 2 Level 3",266,39)
 {
  Outlier ("General",0.05);
 };
 R_Date("VERA-6227_2 maize 335-705 SS25 Midden 2 Level 3",359,34)
 {
  Outlier ("General",0.05);
 };
 R_Date ("OxA-33077 maize 335-705 Midden 2 Level 3", 371,25)
 {
```

```
 Outlier ("General",0.05);
};
R_Date("VERA-6226 maize 335-705 SS25 Midden 2 Level 3",311,33)
{
 Outlier ("General",0.05);
};
R_Date("VERA-6226_2 maize 335-705 SS25 Midden 2 Level 3",324,33)
{
 Outlier ("General",0.05);
};
R_Date("AlGt-66 maize UGA-22311 Sq. 335-705; Midden 2, level 3",270,20)
{
 Outlier ("General",0.05);
};
Date ("Date Spang");
Span ("Span Spang ");
};
Boundary("Mid End Spang")
{
Transition("Duration End Spang");
Start("Start End Spang");
End("End End Spang");
};
Boundary("Mid Start Mantle")
{
Transition("Duration Start Mantle");
Start("Start Start Mantle");
End("End Start Mantle");
};
Phase ("Mantle")
{
R_Date("GrM-13842 144 415-155 F648 Charcoal",469,15)
{
 Outlier ("IA",1);
};
```

```
R_Date("GrM-13844 144 415-155 F648 Charcoal",854,15)
{
 Outlier ("IA",1);
};
R_Combine ("144 415-155 Feature 648 strawberry seeds",8)
{
 Outlier ("General",0.05);
 R_Date("VERA-6212 144 415-155 F648 strawberry seeds",353,37)
 {
  Outlier ("SSimple",0.05);
 };
 R_Date("VERA-6212_2 144 415-155 F648 strawberry seeds",368,38)
 {
  Outlier ("SSimple",0.05);
 };
};
R_Date("GrM-13838 91 535-190 F718 Charcoal",348,15)
{
 Outlier("IA",1);
};
R_Date("GrM-13839 91 535-190 F718 Charcoal",388,15)
{
 Outlier("IA",1);
};
R_Date("GrM-13840 91 535-190 F718 Charcoal",338,15)
{
 Outlier("IA",1);
};
R_Combine ("91 535-190 F718 Maize",8)
{
 Outlier("General",0.05);
 R_Date("VERA-6213 91 535-190 F718 Maize",349,32)
 {
  Outlier ("SSimple",0.05);
 };
```

```
 R_Date("VERA-6213_2 91 535-190 F718 Maize",335,35)
 {
  Outlier ("SSimple",0.05);
 };
 R_Date("OxA-33078 91 535-190 F718 Maize",376,26)
 {
  Outlier ("SSimple",0.05);
 };
 R_Date("OxA-33079 91 535-190 F718 Maize",401,25)
 {
  Outlier ("SSimple",0.05);
 };
};
R_Date("GrM-13834 159 435-180 F427 Charcoal",331,15)
{
 Outlier("IA",1);
};
R_Date("GrM-13835 159 435-180 F427 Charcoal",329,15)
{
 Outlier("IA",1);
};
R_Date("GrM-13837 159 435-180 F427 Charcoal",320,15)
{
 Outlier("IA",1);
};
R_Combine ("159 435-180 F427 Maize",8)
{
 Outlier ("General",0.05);
 R_Date("VERA-6214 159 435-180 F427 Maize",357,36)
 {
  Outlier("SSimple",0.05);
 };
 R_Date("VERA-6214_2 159 435-180 F427 Maize",351,34)
 {
  Outlier("SSimple",0.05);
```

```
 };
};
R_Date("GrM-13833 159 435-180 F427 Strawberry seeds",373,15)
{
 Outlier("General",0.05);
};
R_Date("VERA-6222 20 495-160 F927B Strawberry seeds",361,34)
{
 Outlier ("General",0.05);
};
R_Date("VERA-6225HS 20 495-160 F927B Strawberry seeds",408,33)
{
 Outlier ("General",0.05);
};
R_Combine ("166 400-200 F492 Maize",8)
{
 Outlier ("General",0.05);
 R_Date("VERA-6215 166 400-200 F492 Maize",370,38)
 {
  Outlier("SSimple",0.05);
 };
 R_Date("VERA-6215HS 166 400-200 F492 Maize",333,34)
 {
  Outlier("SSimple",0.05);
 };
 R_Date("VERA-6215_2 166 400-200 F492 Maize",281,34)
 {
  Outlier("SSimple",0.05);
 };
};
R_Date("VERA-6218 164 370-185 F238 Maize",342,36)
{
 Outlier ("General",0.05);
};
R_Date("VERA-6216 126 530-165 F709 Maize",316,34)
```

```
{
 Outlier ("General",0.05);
};
R_Combine ("40 450-120 F1237 Maize",8)
{
 Outlier ("General",0.05);
 R_Date("VERA-6219 40 450-120 F1237 Maize",312,38)
 {
  Outlier("SSimple",0.05);
 };
 R_Date("OxA-33081 40 450-120 F1237 Maize",374,25)
 {
  Outlier("SSimple",0.05);
 };
 R_Date("OxA-33082 40 450-120 F1237 Maize",414,25)
 {
  Outlier("SSimple",0.05);
 };
};
R_Combine ("183 425-135 F468 Maize",8)
{
 Outlier("General",0.05);
 R_Date("VERA-6220 183 425-135 F468 Maize",389,35)
 {
  Outlier("SSimple",0.05);
 };
 R_Date("VERA-6220HS 183 425-135 F468 Maize",351,39)
 {
  Outlier("SSimple",0.05);
 };
};
R_Combine ("36 465-125 F1238 Maize",8)
{
 Outlier("General",0.05);
 R_Date("VERA-6217 36 465-125 F1238 Maize",296,33)
```

```
   {
    Outlier("SSimple",0.05);
   };
   R_Date("VERA-6217HS 36 465-125 F1238 Maize",344,33)
   {
    Outlier("SSimple",0.05);
   };
  };
  Date ("Date Mantle");
  Span ("Span Mantle");
 };
 Boundary ("End Mantle");
};
```